

The fastest routes of approach to dwarf planet Sedna for study its surface and composition at the close range

Vladislav Zubko^{1,2}

¹Space Research Institute, ul. Profsoyuznaya 84/32, Moscow, 117997 Russia,

²Bauman Moscow State Technical University (National Research University), 2nd Baumanskaya ul. 5, Moscow, 105005 Russia

Current research focuses on designing fast trajectories to the trans-Neptunian object (TNO) (90377) Sedna to study the surface and composition from a close range. Studying Sedna from a close distance can provide unique data about the Solar System evolution process including protoplanetary disc and related mechanisms. The trajectories to Sedna are determined considering flight time and the total characteristic velocity (ΔV) constraints. The time of flight for the analysis was limited to 20 years. The direct flight, the use of gravity assist manoeuvres near Venus, the Earth and the giant planets Jupiter and Neptune, and the flight with the Oberth manoeuvre near the Sun are considered. It is demonstrated that the use of flight scheme with ΔV_{EGA} (ΔV and Earth Gravity Assist manoeuvre) and Jupiter-Neptune gravity assist leads to the lowest cost of $\Delta V \approx 6.13$ km/s for launch in 2041. The maximum payload for schemes with ΔV_{EGA} manoeuvre is 500 kg using Soyuz 2.1.b, 2,000 kg using Proton-M and Delta IV Heavy and exceeds 12,000 kg using SLS. For schemes with only Jupiter gravity assist, payload mass is twice less than for ones with ΔV_{EGA} manoeuvre. As a possible expansion of the mission to Sedna, it is proposed to send a small spacecraft to another TNO during the primary flight to Sedna. Five TNOs suitable for this scenario are found, three extreme TNOs 2012 VP113, (541132) Leleākūhonua (former 2015 TG387), 2013 SY99) and two classical KBOs: (90482) Orcus, (20000) Varuna

Keywords: Oort Cloud, trans-Neptunian objects, Sedna, interplanetary mission, gravity assist manoeuvres, Kuiper Belt exploration

1. Introduction

1.1 Astrophysical characterisation of Sedna

Icy bodies placed beyond the orbits of the giant planets are of tremendous interest for studying processes that took place in the earliest stages of the evolution of the Solar System. Some of these bodies (centaurs) are located between the orbits of Jupiter and Neptune. The others are called trans-Neptunian objects (TNOs) because their orbits are beyond the orbit of Neptune. They are classified, according to series of papers [1–5], as objects of the Edgeworth-Kuiper Belt (KBOs) if the semi-major axis (a) > 35 AU, the detached disk ($a > 100$ AU) and the hypothetical Oort Cloud (inner part $a > 500$ AU, and outer part $a > 10,000$ AU). The close-range survey of such bodies should enhance the knowledge of the processes that accompanied the early stages of the Solar System's evolution. Our work, though, focuses on the object that stands out from the rest of TNOs.

TNO (90377) Sedna is a small celestial body whose orbit is located far outside the Edgeworth-Kuiper Belt. Its belonging is a subject of much discussion; because of the remoteness of Sedna, it possibly can belong to the inner Oort Cloud as stated by discoverers [6,7]. Still, the International Astronomical Union (IAU) organization, the Minor Planet Center (MPC) and Small¹ assign Sedna to the scattered disc objects. Observations of Sedna since its discovery in 2004 [1,3,5,8–11] indicate that the object is similar in composition to Pluto and classical KBOs. Such estimates are the reason for the interest in the Sedna because, despite the similarities, its orbit is radically different from most KBOs. In aphelion, it moves away from the Sun at a distance exceeding 1,000 AU and never approaches the Sun nearer than 74 AU at perihelion. Such orbital motion cannot be explained, for example, only by resonance with Neptune caused by the Kozai-Lidov effect as it happens with Pluto and similar objects [8,12]. Nowadays, several celestial bodies have been discovered whose orbits are close to Sedna (sednoids). One of these bodies is, for example, the sednoid 2012 VP₁₁₃ (unofficially named as 'Biden') [4]. The presence of similar orbits of numerous TNOs gives rise to different theories about their origin; the most popular is the theory of scattering objects by the gravity of a massive celestial body, the so-called Ninth Planet hypothesis [13,14]. The ideas of the origin of Sedna are diverse. The discoverers [8] have suggested that Sedna was created in the Solar System at the early stage of its evolution, and its orbit was changed because of the dynamic effects that followed the Sun's formation within a dense stellar cluster [3,8,15–17]. According to other versions, Sedna's orbit was changed by a stellar encounter [4] (e.g., the passing Scholz's star about 70

¹ The IAU MPC official web page. Url: <https://minorplanetcenter.net/data> (Accessed September 17, 2021)

thousand years ago [18] at a distance of 52,000 AU from the Sun), or Sedna had been captured from a low-mass star or a brown dwarf in interstellar space [19].

As of today, observations of Sedna have been carried out only with the help of ground and near-Earth orbital instruments. Observations at wavelengths of 0.4 - 2.4 μm [9,11] as well as over 2.5 μm [9,11] have shown that the surface of Sedna is abundant in ice (>50% [9]) and consists of a mixture of CH_4 , tholin layer, NH_3 , N_2 and H_2O . The assumption of water ice on the surface of Sedna was made from infrared observations using the Infrared Array Camera (IRAC) on the Spitzer Space Telescope at wavelengths above 2.5 μm . The presence of N_2 emission lines in the near-infrared spectrum may indicate the presence of a thin atmosphere in this dwarf planet. Still, such an atmosphere may exist when Sedna moves near the Sun, i.e. ~ 200 yrs out of a 10,500-year orbital period. Paper [20] refers to the possible existence of a subsurface ocean inside Sedna. This theory is explained by the presence of ammonia in concentrations up to 1.4% and the estimated size of the object is from 650 to 1,500 km [9,10,20,21]. The presence of ammonia makes it possible to reduce the melting point of water ice inside Sedna. The object's size makes it possible to judge that at a depth of about 227 km, a 14 km layer of liquid water is warmed by the heat of internal radioactive decay, e.g. ^{26}Al .

The presence of tholins on the surface of Sedna is probably the reason for its bright red colour observed with twin Magellan Baade and Clay 6.5 m telescopes at Las Campanas, Chile and the 8.2 m Subaru telescope atop Mauna Kea in Hawaii [1,9]. In particular, research [1] shows that such colouring is inherent to most Sedna-like objects with aphelion more than 500 AU. According to the same source, the reason for it may be that sednoids stay outside the heliosphere most of the time and are not exposed to the thermal radiation of the Sun. At the same time, the surfaces of long-period comets with a perihelion of the order of 10 AU and an aphelion several orders of magnitude larger than that of Sedna, observed with telescopes, are either blue or red with a spectral gradient (S) <10 (note, the S of Sedna is estimated at ~ 25 units) [1]. This difference in the colouring of the surface of the objects, presumably all having the same origin, may be explained by the intense heating of the surface by the thermal radiation of the Sun during the close approach [1,9–11]. It should also be noted that cosmic rays irradiate Sedna's surface. Therefore, it is interesting to study the interaction of organic compounds and water ice with cosmic rays in the interstellar medium.

The study of the object at close range might considerably enhance the results obtained previously and provide unique data about the early evolution of the Solar System, particularly on the origin of the protoplanetary disk and the mechanisms of its existence.

1.2 Orbit design to Sedna

Researches toward studies of a flight to Sedna began since 2011. The paper [22] defines the best scenario of reaching Sedna with a single Jupiter gravity assist (JGA). According to [22], such a flight would require a total cost of 7.42 km/s of characteristic velocity (ΔV) and a time of flight (TOF) of 24.48 yrs. It is worth highlighting the studies carried out in the paper [23], which considers flight scenarios to Varuna, Haumea, Makemake, Ixion and Sedna. The research carried out in papers [23,24] showed that increasing ΔV and using JGA makes it possible to reach Sedna in 18-20 years of TOF. However, their estimate of necessary ΔV was about 14.5 km/s.

A flight to Sedna for the subsequent insertion into the orbit of its satellite would require both a large launch ΔV and a braking impulse because the mass of Sedna is small and the velocity of the spacecraft, acquired through gravity assist manoeuvres, is too high. Estimates of orbiting Sedna using high thrust are given in [23]. Therefore, the only way to study Sedna becomes its observation from a flyby trajectory. Note, the authors of the paper [24] considered the flight to Sedna with electric propulsion (low thrust) and braking to a satellite orbit of Sedna. According to them, the orbiting Sedna is possible, using low thrust, and the mass of the satellite can be about 50-100 kg if heavy or super-heavy launch vehicle is used [24].

Only one mission in history is known to have successfully explored TNOs at close range. New Horizons successfully explored Pluto and the TNOs (486958) Arrokot from a flyby trajectory. Based on this mission data, several good objectives for the study of Sedna can be highlighted [25–28], as follows:

- Sedna surface spectrometry;
- the presence of a magnetic field of the object;
- investigation of the effect of solar wind and interstellar radiation on organic compounds (tholins), water ice on the surface of the object;
- study of the presence of an atmosphere;
- testing the hypothesis of a subsurface ocean (via impact mission/using descent probes or capsules, or sending the spacecraft to the near Sedna orbit);
- surface composition study by taking a sample of the Sedna soil ejected by means of hitting the surface by a projectile separated from the spacecraft before the Sedna encounter;
- clarification of the mass of the object [29];

- obtaining images of Sedna in the optical range, conducting photo and video study sessions of the object;
- studies of the dust composition of the Kuiper Belt;
- specific studies of the solar wind at long distances from the Sun.

The papers [30–38], which consider scenarios of flights to other TNOs and, in particular, to the interstellar body 1I/Oumuamua [30–32], are also of interest. The authors of [35] analyse the application of tether systems for a flight to Haumea and other Edgeworth-Kuiper Belt objects. In [23], the use of the JGA and other gravity assists for the flight to 45 TNOs are analysed. In their work on the flight to the 1I/Oumuamua asteroid, the authors examine the use of predominantly flight schemes, including the Oberth manoeuvre near the Sun [31,39]. Due to the close approach to the Sun, a small impulse in the vicinity of the perihelion allows to significantly increase the heliocentric velocity of the spacecraft [39]. The results show that it is possible to reach 1I/Oumuamua at a distance of 70 to 110 AU with such an approach. The cost of such flight will be from 15 to 30 km/s within TOF from 18 to 22 yrs correspondingly [31]. Research [39–42] of interplanetary and interstellar flight using laser solar sail and direct fusion drive is worth mentioning. The results given in [41] show that, for example, a flight to Haumea, Makemake and Eris will only take 6 to 10 yrs at a propellant consumption of about 3.5–4 tonnes.

In the works [43,44], trajectories to Sedna were determined satisfying two constraints simultaneously, namely, with the TOF no longer than 50 yrs, the total characteristic velocity (ΔV_{Σ} that is the sum of the characteristic velocity required for launch, as well as all manoeuvres in deep space and near planets) had to be less than 8 km/s. In all cases, the correcting manoeuvres were not considered since they depend on the navigation and the manoeuvres execution accuracy. Thus, the problem of the flight to Sedna was reduced to the search of the minimum ΔV_{Σ} under the restrictions on the TOF.

The current work focuses on the search for flight schemes to Sedna, ensuring the fastest way to reach it under the only restriction on ΔV_{Σ} being the natural limitation of the chemical propulsion systems. Because of this, flights restricted on duration to 10–20-yr are considered, that is admissible because the average time of satellite's lifetime is evaluated approximately in 15 yrs. On the other hand, all previous missions to deep space such as Pioneer 10, Pioneer 11, Voyager 1, Voyager 2, Galileo, Ulysses, New Horizons and others lasted at least 5–10 yrs before they fulfilled their main goal of the mission. Also, the additional problem that is to find the TOF which corresponds to the limited ΔV_{Σ} was considered in this paper. Note that in all flight schemes to Sedna that will be analysed in this paper the costs of orbit correction manoeuvres are not considered, as well as in the paper [43].

Note that the trajectory analysis was done only for high thrust, because the main objective of this paper is to demonstrate that it is possible to reach Sedna by well-known means, even when the time of flight is severely limited. In addition, low thrust has a significant disadvantage seen in a flight to such a distant object as Sedna. Namely, since the effectiveness of the thrust decreases with increasing the distance from the Sun (correct for solar electric propulsion (SEP)), using low thrust beyond Jupiter's orbit does not seem to be a feasible option. In such a case, the use of a fusion engine, a nuclear power plant or a laser solar sail may be considered for a flight to Sedna, but this subject requires special consideration.

This research analyses direct flight in order to compare it with more complex schemes involving gravity assist manoeuvres. Particular attention is given to flight schemes with active manoeuvres (i.e. extra ΔV costs are needed) in deep space and scheme with an Oberth manoeuvre (OM) near the Sun. Strategies with gravity assist manoeuvres include ones at both Venus and Earth and giant planets. Approximate estimates of the payload mass delivered to Sedna are given.

A possible expansion of the mission to Sedna has also been proposed. In such a scenario, a flight takes place simultaneously to both Sedna and another TNO by separation of a small probe from the spacecraft. Such separation takes place during the Jupiter or Neptune flyby. After that the probe is directed to another TNO, the flight to which is possible without additional manoeuvres in the planetary sphere of influence (SOI). Results are given for five TNOs suitable for this scenario, including three extreme TNOs 2012 VP₁₁₃, (541132) Leleākūhonua (former 2015 TG₃₈₇) and 2013 SY₉₉ and two classical KBOs: (90482) Orcus, (20000) Varuna.

2. Direct flight to Sedna

First, it is essential to study a direct flight to the object since such a flight has the most remarkable simplicity in terms of orbit construction and control of the spacecraft as it moves towards the target. Also, a direct flight is essential for determining the basic energy characteristics of the trajectories, namely the required cost ΔV depending on the launch and arrival dates. The value of the required ΔV is determined by solving the Lambert problem. The point of this boundary value problem is to define the spacecraft's orbit in the framework of the Kepler motion model

according to two given positions and the time of spacecraft flight between these positions. There are many methods for solving this problem; in this paper, we use [45,46], which are based on a universal variable.

To analyse the direct flight, we plot the ΔV vs launch and arrival dates for flight to Sedna (Fig. 1).

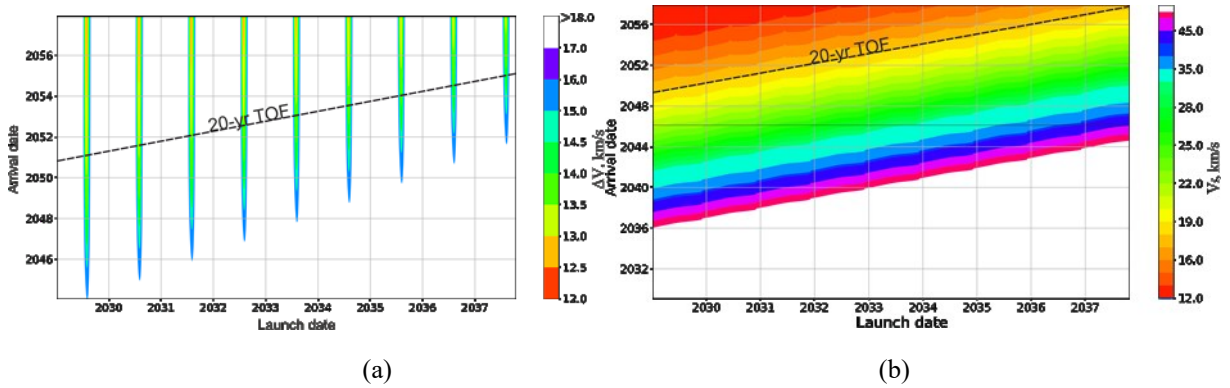


Fig. 1 (a) - ΔV vs launch and arrival dates to Sedna, (b) – spacecraft's rendezvous velocity with Sedna (V_r) vs launch and arrival dates to Sedna.

The ΔV value (Fig. 1a) show that its value for the flight to Sedna cannot be less than 14.5 km/s for the TOF less than 20-yr. This value of the launch ΔV (ΔV_0 in this section equal to ΔV) for a flight to Sedna will require to use super-heavy launch vehicle with at least 3-4 additional stages.

Note that the value of the spacecraft velocity of Sedna flyby (V_f) (Fig. 2b) is exceeds 15 km/s for a 20-yr flight what is too high. Since the gravitational parameter of Sedna is small, the impulse required for the spacecraft to enter the orbit of the satellite of Sedna will be approximately equal to the relative velocity of the spacecraft. It means that the total cost for launch and breaking to the orbit of Sedna will be at least 29 km/s, which is currently quite fantastic, rather than a realistic value of the characteristic velocity when planning a direct mission with a final insertion to the orbit Sedna satellite.

3. The fastest routes to Sedna using gravity assist manoeuvres

3.1 Methods of trajectories calculation

In this work, the patched conic approximation [47–51] is used as a model of spacecraft motion. In this approximation, it is supposed that during the spacecraft flight in the planets' SOI, the spacecraft motion is affected only by the gravity force of the central body and beyond the SOI (i.e. on the heliocentric arc) influenced only by the gravity force of the Sun. In other words, all perturbing forces, including solar radiation pressure, oblateness, attraction of other planets on the spacecraft motion, are neglected. While the spacecraft moves inside the SOI, its size is considered infinite, i.e. the planetocentric velocity of the spacecraft on the SOI boundary is assumed to be equal to its asymptotic velocity. As for the heliocentric trajectories, the planetary SOI are considered point ones permissible at the first step of trajectories design considering the size of the planets SOI compared to heliocentric distances. Therefore, the n-body problem is reduced to a set of two-body problems; a solution of each of them is a Keplerian orbit (i.e., a conic section). The problem is to find these orbits and to patch them into a whole trajectory [52].

The parameters of arrival and departure heliocentric arcs are determined using the Lambert problem solution. In the next step, they are connected in their pericenters, so that their heights are equal and tangents coincide. The magnitude of the difference of the velocity vectors at the pericentre of these hyperbolas is equal to the impulse ΔV needed to connect the trajectory's arrival and departure arcs. If the planet's gravitational field is incapable of turning the asymptotic velocity vector from its incoming direction to the outgoing one, an additional impulse rotating the velocity vector to the necessary direction is required.

A two-step procedure is used to search for optimal trajectories, i.e. trajectories that ensure a minimum ΔV_Σ under the given constraints. In the first step, the minimum is calculated using a differential evolution (i.e. a part of genetic algorithms family). The differential evolution belongs to the family of metaheuristic algorithms of the extremum search [53,54]. The extremum of the function ΔV_Σ is determined within the limits of imposed constraints on the heliocentric TOF. In general, the method makes it possible to identify the vicinity of the global minimum of the function under sufficiently loose restrictions on the TOF between the celestial bodies. On the second stage of procedure modification of the Broyden-Fletcher-Goldfarb-Shanno algorithm (BFGS), namely L-BFGS-B algorithm (L is addressed to the limited memory and B is the bound constraint) [55] is used for the precise determination of the function minimum. Note, the algorithm has used the gradient with curvature information for defining direction to a minimum, gradually improving an approximation to the Hessian matrix obtained numerically.

Let us limit the TOF for flight to Sedna, as follows:

$$TOF \leq 20 \text{ yrs} \quad (1)$$

Emphasise that constraint (1) is acceptable considering that to date, the lifetime of the spacecraft in-orbit is about 15-yr [56,57]. Note that value of constraint (1) is used directly in the optimisation process. Limit on the value of ΔV_{Σ} will be given further, considering the upper stage's physical (real) characteristics. Note, there would also be used a natural restriction that is the minimum flyby height; by default, this height was taken equal to 5% of the planet radius. Such height was taken because we sought to obtain a maximum gain of the gravity assist keeping the flyby distance in a safe range of any collisions with the planet in the search process.

The application of the described approach to finding optimal trajectories allows to simplify the optimisation process greatly and, at the same time, to obtain good initial approximations for more accurate calculations [49]. The results of [49,60] show that the difference between the minimum ΔV values obtained using the patched conic approximation and the accurate n-body problem solution is relatively small. However, the launch and flybys dates that correspond to the values may be slightly different [49].

3.2 Analysis of JGA for flight to Sedna

Voyages outside the heliosphere are more feasible using the advantages of the gravitational fields of the giant planets. Since Jupiter is the most massive planet, its gravity allows getting the most significant increase in orbital energy of the spacecraft. Several flight schemes to Sedna including assist of this giant planet will be considered below.

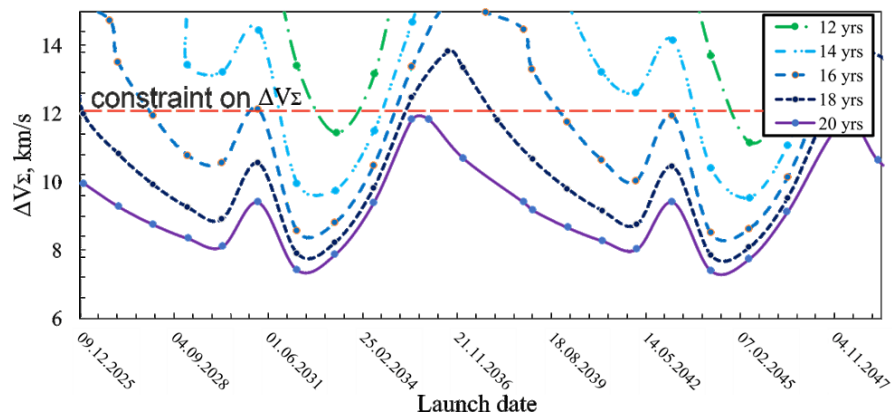
An advantage of the Earth-Jupiter-Sedna (EJSed) scheme compared to the schemes that would be described below is that EJSed requires lesser gravity assists, which decreases the additional fuel cost of the trajectory corrections during the passage of celestial bodies. On the other hand, a significant disadvantage of such a flight is that the decreasing of ΔV_{Σ} is lesser among the other schemes. Fig. 2 shows the ΔV_{Σ} and the flyby velocity of the spacecraft at Sedna (V_f) vs TOF at launch windows from 2025 to 2050.

It is possible to limit ΔV_{Σ} , as follows:

$$\Delta V_{\Sigma} \leq 12 \text{ km/s} \quad (2)$$

This restriction is provided by taking the maximum allowable ΔV of 3.5 km/s for one interplanetary stage (7 km/s for the set of two stages) with a specific impulse of ~308-320 s and by launch vehicle upper stage ΔV of ~4.5-5 km/s (the specific impulse of about 355 s). For all the manoeuvres, it is supposed to use asymmetrical dimethylhydrazine as fuel and nitrogen (II) tetraoxide as oxidiser because these components provide specific impulse of about 310 s.

Note that the restriction (2) is not practically achievable since there have not yet been missions in which such a ΔV_{Σ} value has been used. However, for our analysis, this value is important as the filter (i.e. not limited directly into optimisation process) whose purpose is to remove trajectories with a deliberately high ΔV_{Σ} value and reduce the number of analysed flight schemes.



(a)

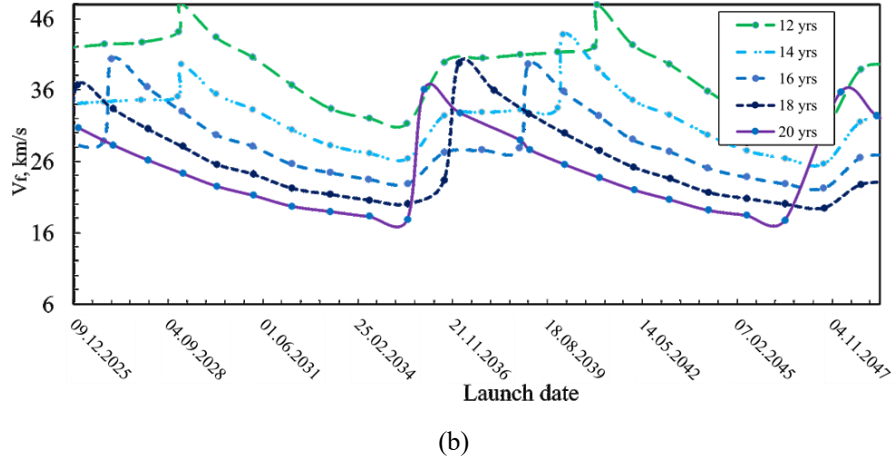


Fig. 2 (a) ΔV_{Σ} for 12; 14; 16; 18 and 20-yr TOF vs. launch dates, (b) V_f curves for 12; 14; 16; 18 and 20-yr TOF vs launch dates.

Looking through the obtained ΔV_{Σ} profiles in Fig. 2, it is seen that the best launch year is 2032, in which the low V_f value is also obtained (18.9 km/s). The minimal V_f is reached in 2035 and amounts to 17.9 km/s in a 20-yr TOF. If we limit the TOF to 15-yr, the best year changes to 2033 providing the launch ΔV of 9.3 km/s.

Note the spacecraft flyby Sedna with a high velocity V_f (minimum 17.9 km/sec). Let us give the main reasons for such value of approaching velocity by comparing the mission to Sedna with the New Horizons. In the New Horizons mission [25], the spacecraft passed Pluto at a velocity of 13.7 km/s (distance to Sun of about 30 AU). In our case, however, the speed is 18 km/s or more. If we consider that New Horizons reached Pluto in 9 years at 13.7 km/sec, it takes about 25 years to reach a distance of 80-85 AU. In all the cases considered, reaching Sedna (distance to Sun of about 80 a.u.) is assumed to take 20 years or less. Therefore, the main reason for the high flyby velocity of Sedna is, first of all, a restriction on the flight time. Note, however, that the number of gravity assist maneuvers also has an effect. Since the orbital energy of the spacecraft relative to the Sun will increase (in this case), the approach velocity will also naturally increase, which is confirmed by the data of the tables of Appendix A.1-A.6.

Note that the magnitude of ΔV_{Σ} is almost entirely repeated every 12 years, i.e. through the orbital period of Jupiter. Such repetition is explained by the fact that Sedna moves only by a small angle on the celestial sphere during a complete revolution of Jupiter and the primary and decisive influence on changes in the dynamics of ΔV_{Σ} is affected by the mutual position of the Earth and Jupiter, at least during several decades. However, as can be seen from Fig. 2 (a), practically in the vicinity of a ΔV_{Σ} minimum, namely in 2031 and 2033, there is a rough rise of ΔV_{Σ} . This rough increase is most probably caused by the fact that in these years the angular distance of flight by Earth-Jupiter segment appears to be close to the 180 deg. Because the orbits of the Earth and Jupiter are not coplanar, a considerable increase in the heliocentric orbit inclination (up to more than 7 degrees to the ecliptic) is required. That is possibly the reason for an increase in ΔV_{Σ} curves in Fig 2.

The detailed catalogue of selected trajectories for different TOF is given in Appendix A, Table A.1. In Fig. 3 the spacecraft's trajectory to Sedna by EJSed scheme at launch in 2032 for 17-yr TOF is shown. The spacecraft trajectory parameters using EJSed scheme for the launch in 2032 are shown in Table 1.

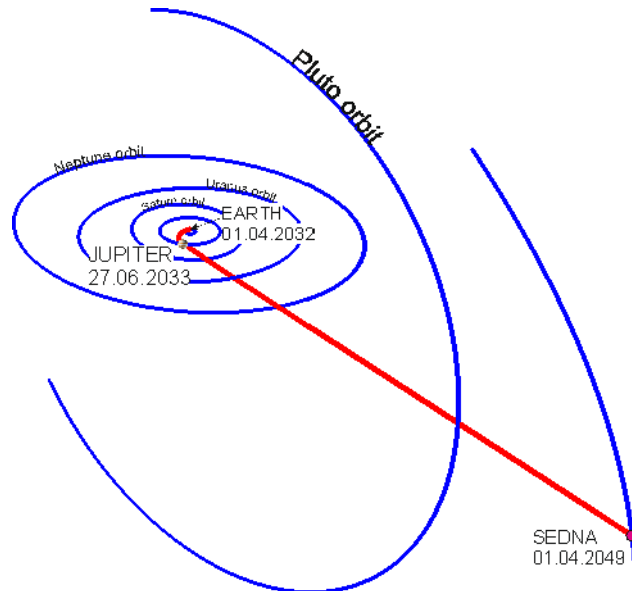


Fig. 3 Trajectory of the spacecraft flight to Sedna by EJSed scheme at launch in 2032

Table 1 The spacecraft trajectory parameters using EJSed scheme for the launch in 2032

Celestial bodies	Dates of Launch and flyby of celestial bodies, dd.mm.yyyy	Relative velocities near-Earth and of the flyby of celestial bodies, km/s	ΔV of launch, at aphelion and of the flyby of celestial bodies, km/s	Height of the initial orbit and flyby above celestial bodies, 10^3 km
Earth	01.04.2032	10.93	7.73	0.2
Jupiter	27.06.2033	16.35	0.48	4.7
Sedna	01.04.2049	23.77	-	0.0*

* Approaching an object is assumed to be at any small distance

3.3 Flight to Sedna with AVEGA manoeuvre

It is possible to use the manoeuvre $\Delta V_{\text{AVEGA}} = \Delta V$ and Earth Gravity Assist, where ΔV is a small braking impulse in the vicinity of the aphelion on the Earth-Earth loop (ΔV_a) to reduce the cost of the characteristic velocity at the stage of flight to Jupiter. The deceleration at aphelion leads to some increase in the relative velocity during the Earth flyby and enables a significant reduction of ΔV in the trajectory part Earth-Jupiter.

A study of the flight to Sedna is performed for the Earth- ΔV_a -Earth-Jupiter-Sedna (E ΔV_{EJSed}) scheme compared to the EJSed scheme. Note that the duration of the Earth-Earth trajectory part is determined in the optimisation process by the condition of minimum total ΔV required for flight to Sedna. In terms of satisfying constraints (1) and (2), the E ΔV_{EJSed} scheme is similar to the EJSed one. Only for launch in 2033, 2034 and 2046, the fulfilment of constraint (2) for E ΔV_{EJSed} scheme is violated (Fig. 4). However, for launch dates 2029 to 2031 and 2035 to 2040, the use of E ΔV_{EJSed} scheme reduces the total ΔV cost by 1-2 km/s (Fig. 4).

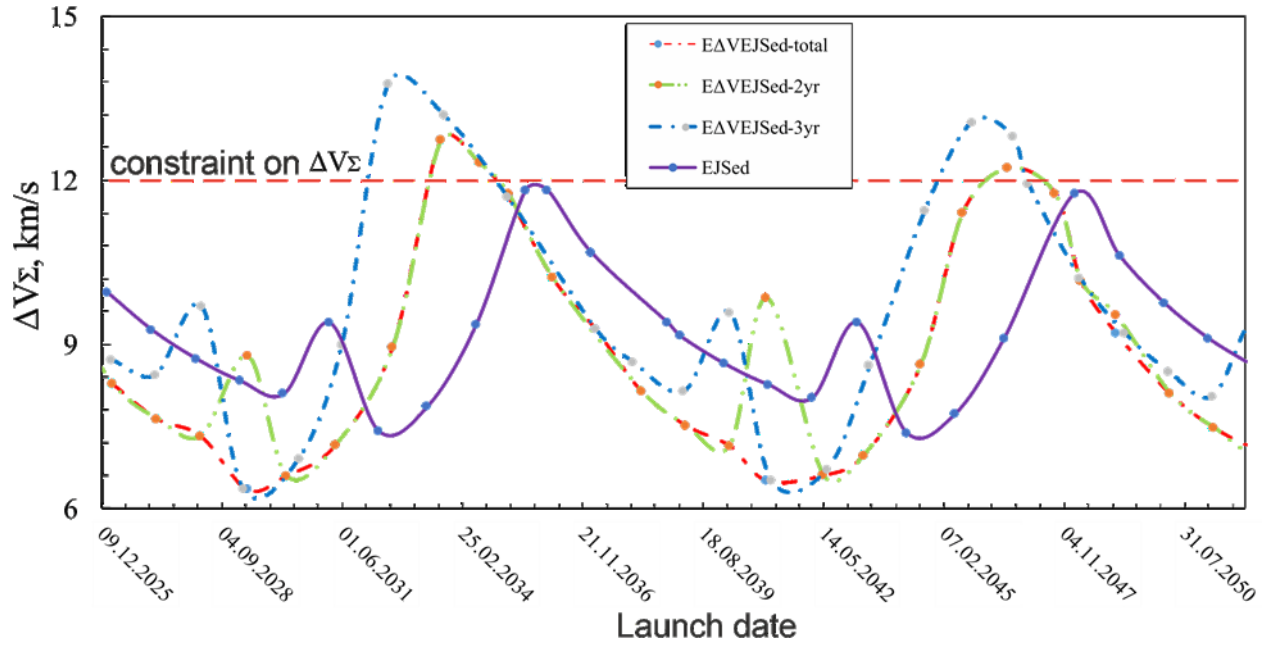


Fig. 4 Comparison of ΔV_{Σ} vs launch year using EJSed and EΔVEJSed schemes for 20-yr TOF. In the figure the EΔVEJSed scheme was separated on the EΔVEJSed-2yr, which corresponds to the 2-yr flight on Earth-Earth (E-E) section, EΔVEJSed-3yr which corresponds to the 3-yr on the E-E trajectory part and EΔVEJSed-total which consists from the best solutions obtained for 2-yr and 3-yr flight on the E-E trajectory part.

ΔV_{Σ} vs TOF for the launch dates within 2029-2031 given in Fig. 5. The launch dates from 2029 to 2031 require more detailed consideration since these dates are in the vicinity of ΔV_{Σ} minimum (Fig. 4). Launch in 2029 allows reducing the ΔV_{Σ} to ~ 9 km/s for the 16-yr TOF and to 6.29 km/s for the 20-yr TOF. Such results are comparable with ones obtained in [43,61] for the more complex Earth-Venus-Earth-Earth-Jupiter-Sedna (EVEEJSed) scheme ($\Delta V_{\Sigma} = 6.27$ km/s in 2029). Notice that the launch date in 2028 is also in the vicinity of the ΔV_{Σ} minimum. Still, as it was stated earlier, it makes no practical sense to consider flights before 2029 since the preparation and performance of the mission to Sedna may take more than one decade.

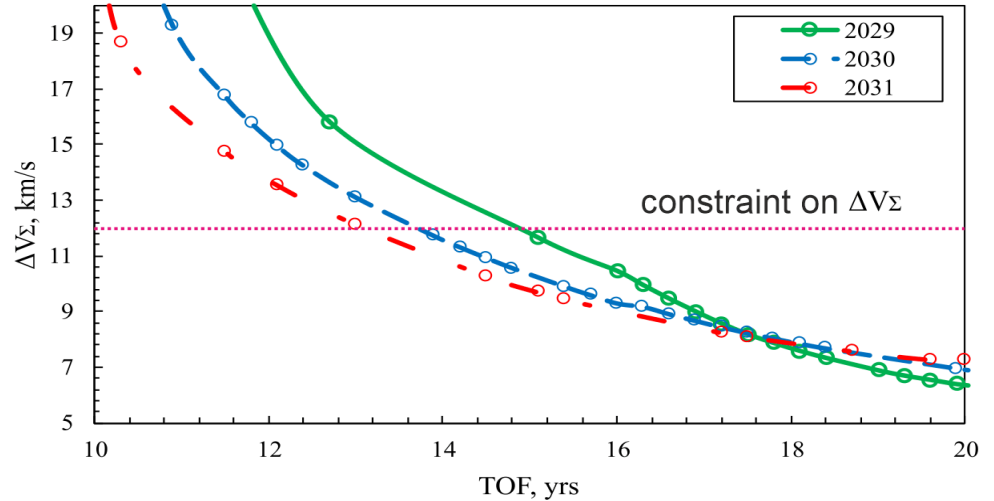


Fig. 5 ΔV_{Σ} vs TOF for flight to Sedna using EΔVEJSed scheme at launch in 2029-2031.

The ΔV_{Σ} curve presented in Fig. 5 shows that the flight to Sedna considering the constraint (2) is achieved for the TOF of 14-14.5 years. A TOF over 16 years will require $\Delta V_{\Sigma} \approx 9$ km/s similar to the New Horizons [58]. Note that the considered launch years in Fig. 5 TOF of about 17.5 years corresponds to the ΔV_{Σ} cost is equal to 8.1 km/s.

In Appendix A, Table A.2, the best results for EΔVEJSed for launch from 2029 to 2042 (one orbital period of Jupiter), satisfying the constraints (1) and (2), are shown. The spacecraft trajectory by the EΔVEJSed scheme to Sedna in 2029, with a 17-yr TOF, is shown in Fig. 6. The spacecraft trajectory parameters using the EΔVEJSed scheme at launch in 2029 are shown in Table 2.

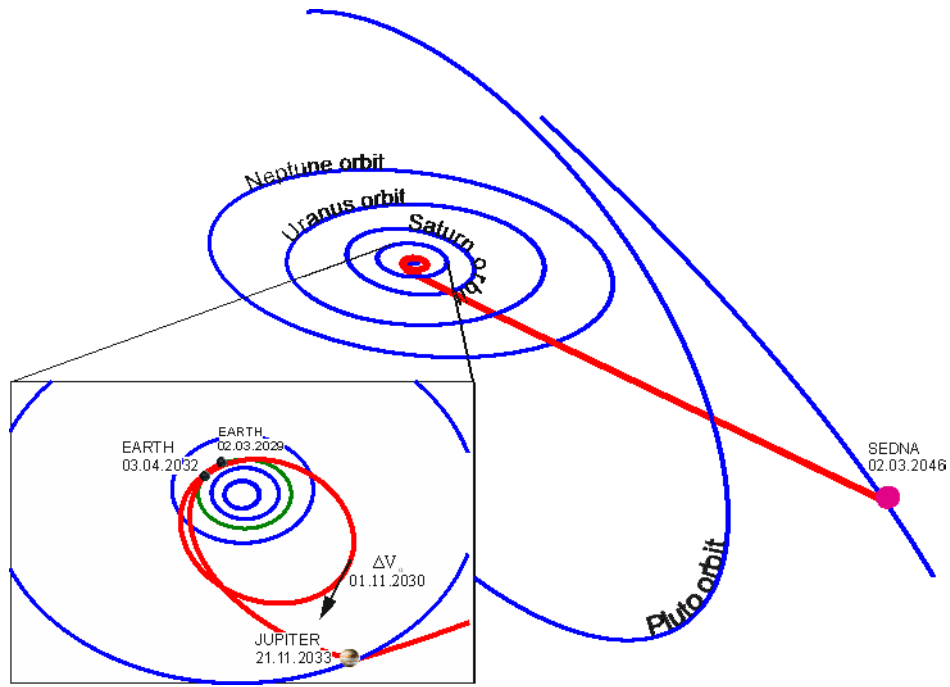


Fig. 6 Spacecraft trajectory to Sedna by EΔVEJSed scheme at launch in 2029

Table 2 The spacecraft trajectory parameters using EΔVEJSed scheme for launch at 2032

Celestial bodies	Dates of Launch and flyby of celestial bodies	Relative velocities near-Earth and of the flyby of celestial bodies, km/s	ΔV of launch, at aphelion and of the flyby of celestial bodies, km/s	Height of the initial orbit and flyby above celestial bodies, 10^3 km
Earth	02.03.2029	6.94	5.24	0.2
ΔV_a	01.11.2030	11.33	0.25	-
Earth	03.04.2032	9.54	0.00	2.7
Jupiter	21.11.2033	21.70	3.37	3.6
Sedna	02.03.2046	30.53	-	0.0*

* Approaching an object is assumed to be at any small distance

3.4 Gravity assist of Neptune in manoeuvre ΔVEGA for the voyage to Sedna

The expansion of the expedition to Sedna by the additional study of the planets and many of their moons from the flyby trajectory is of particular interest. Of course, such an extension of the mission should not increase TOF and ΔV costs. Studies considering the expansion of gravity assist scenarios have already been made in [23,43]. It has been shown that due to the orbital positions of Uranus and Sedna, the gravity assist of Uranus is entirely impossible in the next few decades. On the other hand, using Saturn is possible only at the flight duration of 33-yr or more [43]. However, in [43] in the number of schemes Neptune flyby allows reducing the value of ΔV_{Σ} significantly, and in some cases allows increasing the altitude of the Jupiter flyby, what is also important.

The current paper considers the use of the Earth-Jupiter-Neptune-Sedna (EJNSed) and Earth- ΔV -Earth-Jupiter-Neptune-Sedna (EΔVEJNSed) schemes. The first scheme slightly improves the EJSed scheme, while the second scheme combines the advantages of ΔVEGA, JGA, and Neptune's gravity assist.

Let us first consider the EΔVEJNSed scheme. Fig. 7 shows the ΔV_{Σ} vs launch date for 20-yr and 30-yr TOF using the EΔVEJNSed scheme and only for 20-yr TOF using the EJSed scheme. The results for the EJSed scheme are given to compare both schemes by the ΔV_{Σ} value.

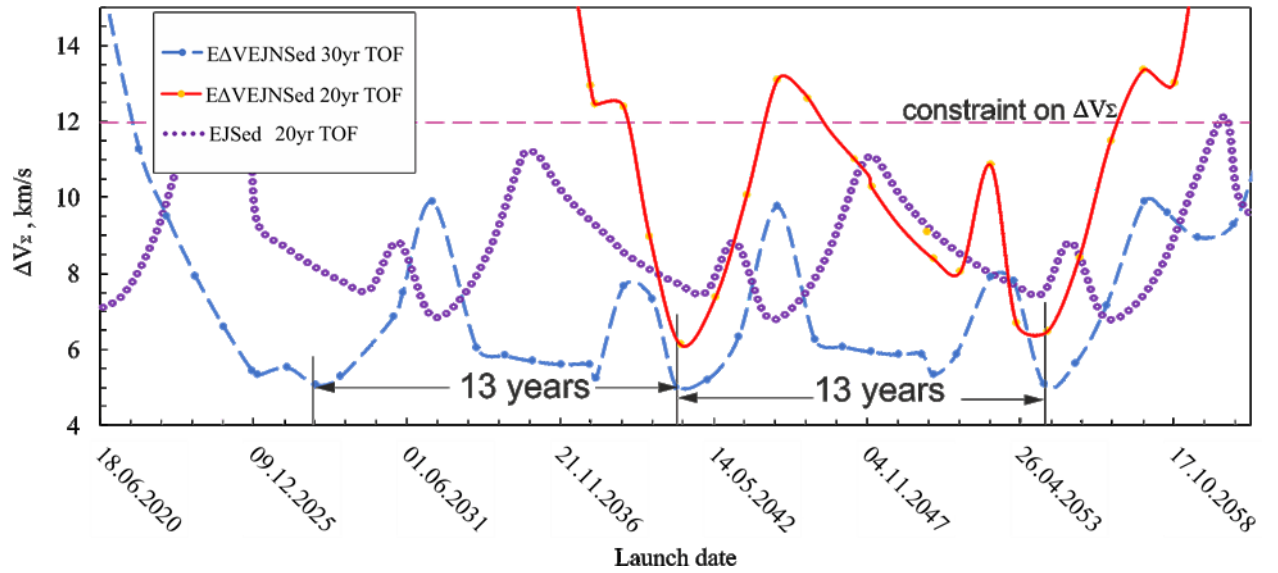


Fig. 7 ΔV_{Σ} vs launch date for EΔVEJNSed scheme for TOF of 20 and 30 yrs

In the considered launch date interval from 2029 to 2040, the use of the EΔVEJNSed scheme under the constraint (1) does not give a significant gain compared to the EJSed and EΔVEJNSed schemes. Still, in 2041, the EΔVEJNSed scheme may be the best for 20-yr TOF among other considered schemes, including ones in the papers [43]. Such result cannot be due only to a random coincidence of the lucky orbital positions of the Earth, Jupiter, Neptune and Sedna, i.e. there must be a regularity of the appearance of such minima. And such explanation has been found. In the research of Alexander A. Sukhanov,² the calculation of the repeatable configuration for any number of planets was considered. For the combination of Earth, Jupiter and Neptune a period of repeating their mutual positions of 1, 12 and 13 yrs was obtained, depending on the required accuracy of the calculation. It is easy to see that a flight using gravity assists of these planets is possible every year following the abovementioned results. However, in this problem, the influence of the position of Sedna relative to Jupiter and Neptune seems to be the decisive factor, so a low-cost flight is not possible every year. However, the recurrence frequency of minimum cost ($\Delta V_{\Sigma} = 6.13$ km/s in 2041) is achievable every 13 years. A confirmation of this result is the flight in 2054 (Fig. 7), the minimum cost ΔV_{Σ} for which will be about 6.48 km/s. The flight in 2028 can also be performed with costs comparable to those of 2041 but with a TOF of at least 30 years (Fig. 7).

A catalogue of trajectories using EΔVEJNSed scheme and satisfying (1) and (2) is given in Appendix A, Table A.3. The spacecraft trajectory by EΔVEJNSed scheme to Sedna in 2041, with an 18-yr TOF, is shown in Fig. 8. The spacecraft trajectory parameters using the EΔVEJNSed scheme at launch in 2041 are shown in Table 3.

² His paper “Repeatability of a given configuration of planets” is in preparation.

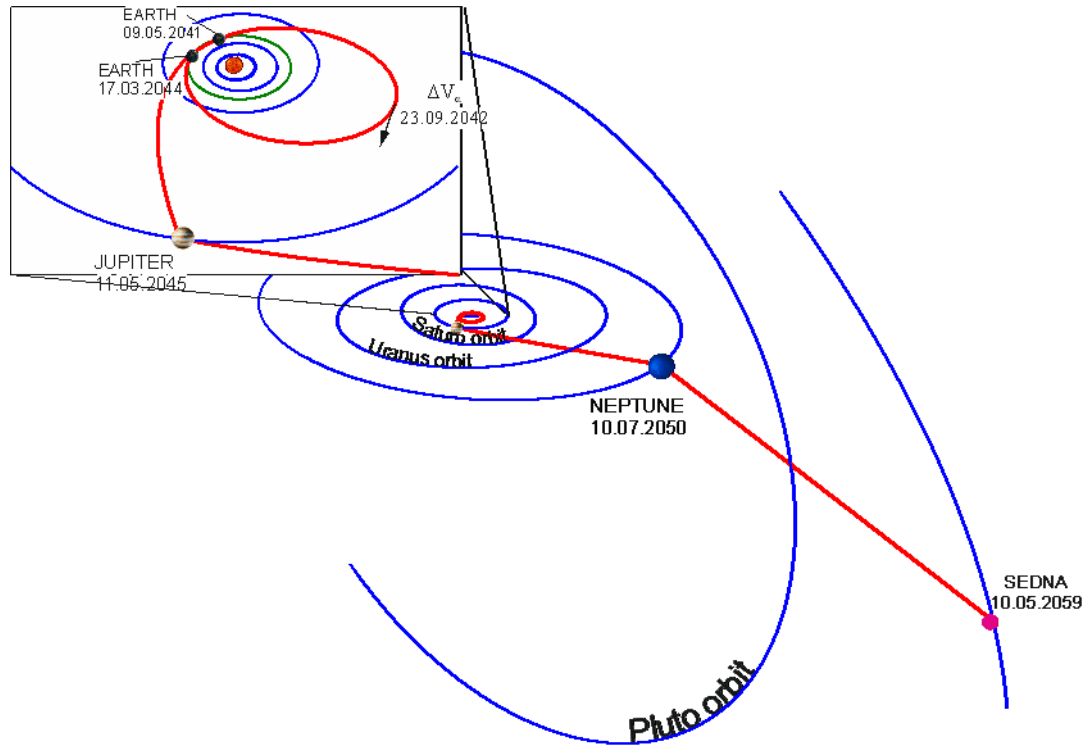


Fig. 8 Trajectory of the spacecraft flight to Sedna in the EΔVEJNSed scheme at launch in 2041.

Table 3. The spacecraft trajectory parameters using EΔVEJNSed with the TOF of 18-yr

Celestial bodies	Dates of Launch and flyby of celestial bodies	Relative velocities near-Earth and of the flyby of celestial bodies, km/s	ΔV of launch, at aphelion and of the flyby of celestial bodies, km/s	Height of the initial orbit and flyby above celestial bodies, 10^3 km
Earth	09.05.2041	7.05	5.30	0.2
ΔV_α	23.09.2042	11.14	0.57	-
Earth	17.03.2044	13.31	1.01	0.3
Jupiter	11.05.2045	17.79	0.32	42.6
Neptune	10.07.2050	25.59	1.81	1.2
Sedna	10.05.2059	27.90	-	0.0*

* Approach to the object is assumed to be at any small distance

3.5 Gravity assist of Neptune in Earth-Jupiter-Sedna voyage

It is almost impossible to perform a flight using EJNSed for launch dates up to 2039 under the constraints (1) and (2), as shown in Fig. 9. However, for launch dates from 2040 to 2060, a few launch windows ensuring minimum ΔV_Σ satisfying constraint (2) are found (Fig. 9).

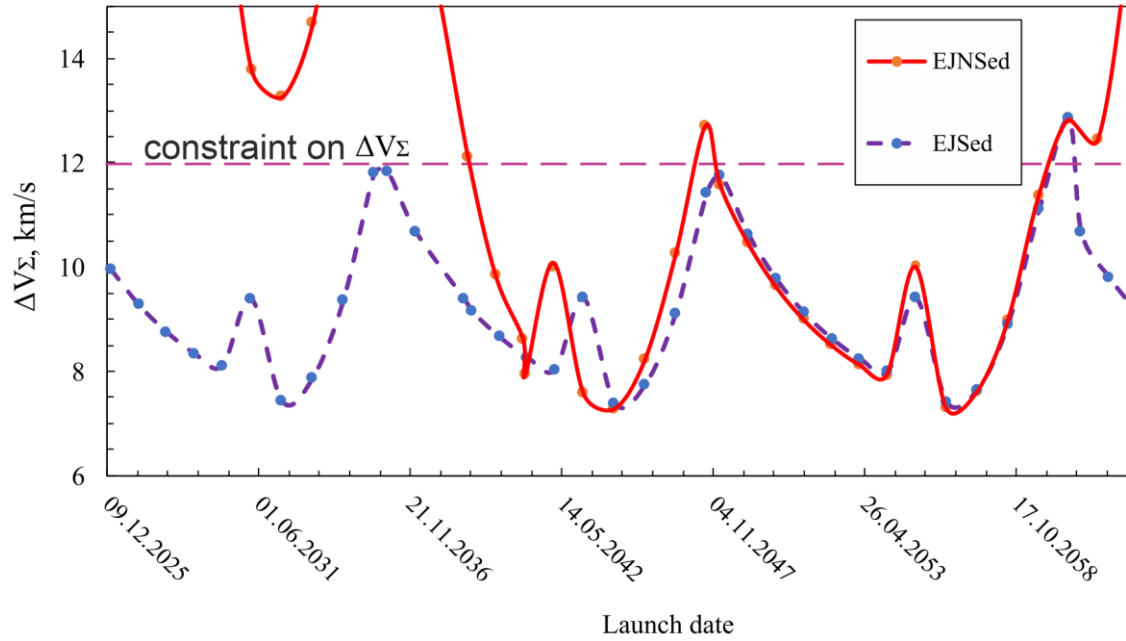


Fig. 9 Comparison of ΔV_{Σ} for 20-yr of TOF vs launch dates for EJSed and EJNSed schemes.

The EJNSed flight for 20-yr TOF shows no significant advantages comparing with the EJSed scheme (Fig. 9). Using the EJNSed scheme at launch in 2041 allows reducing the ΔV_{Σ} value on 330 m/s compared with the EJSed scheme. The period of repeatability of the ΔV_{Σ} is equal to 13 years and is the same as for the previously discussed E Δ VEJNSed scheme.

Table A.4 (Appendix A) contains a catalogue of selected trajectories to Sedna using the EJNSed scheme. In Fig. 10, the trajectory to Sedna using the EJNSed scheme at launch in 2044, with a duration of 20-yr is shown. The trajectory characteristics of the flight to Sedna using the EJNSed scheme are shown in Table 4.

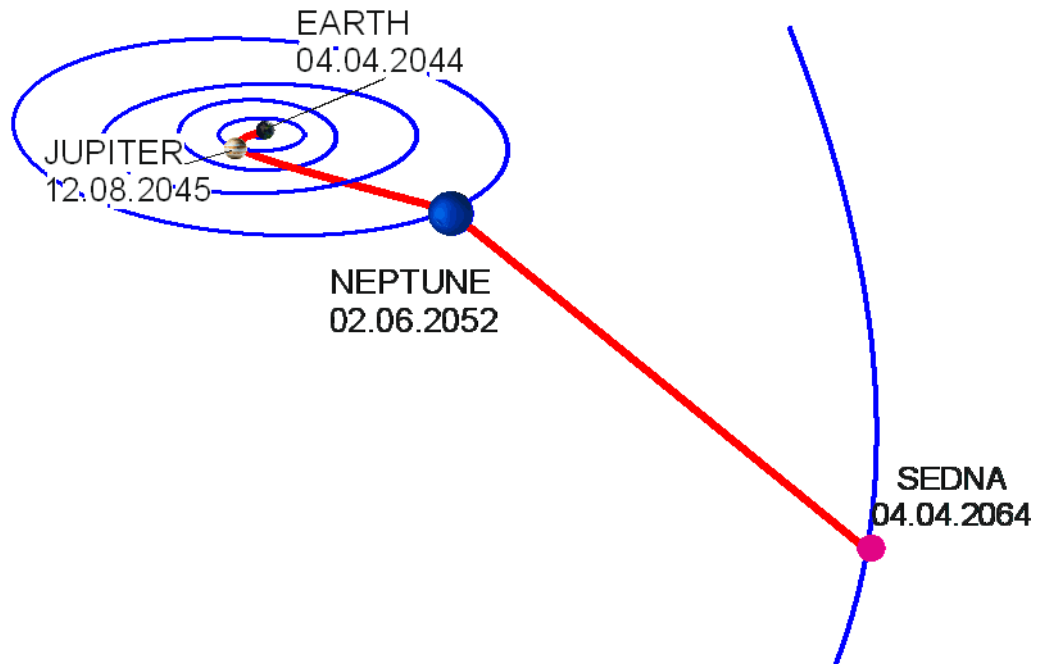


Fig. 10 Spacecraft trajectory to Sedna using the EJNSed scheme for launch in 2044

Table 4. The spacecraft trajectory parameters using EJNSed scheme for launch in 2044 with the 18-yr TOF

Celestial bodies	Dates of Launch and flyby of celestial bodies, dd.mm.yyyy	Relative velocities near-Earth and of the flyby of celestial bodies, km/s	ΔV of launch, at aphelion and of the flyby of celestial bodies, km/s	Height of the initial orbit and flyby above celestial bodies, 10^3 km
Earth	04.04.2044	10.29	7.29	0.2
Jupiter	12.08.2045	12.58	0.00	232.4
Neptune	02.06.2052	18.43	0.00	20.0
Sedna	04.04.2064	20.34	-	0.0*

* Approach to the object is assumed to be at any small distance

3.6 Remark on the VEEGA and VEΔVEGA manoeuvres in the problem of the fastest approach to Sedna

In the paper [43], the authors considered the use of different flight schemes to Sedna based on the VEEGA (Venus-Earth-Earth Gravity Assist) manoeuvre or its modification VEΔVEGA (modification of VEEGA with breaking ΔV in the aphelion of Earth-Earth loop) at the launch dates in 2029-2034. An advantage of these schemes is that in some cases the flight would only require ΔV necessary for the flight to Venus. However, the TOF interval of 20 to 50 yrs adopted by the authors [43] does not fully evaluate the effectiveness of this approach in finding the fastest route to reach Sedna under the constraints (1). For this reason, in the current paper the ΔV_{Σ} vs TOF was plotted for the launch in 2029 only for the interval of TOF from 10 to 20 yrs (Fig. 11).

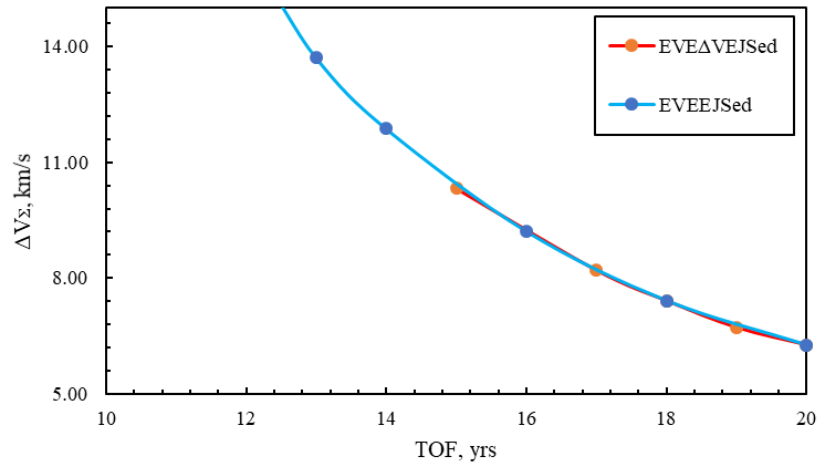


Fig. 11 ΔV_{Σ} vs TOF for flight to Sedna using EVEEJSed and EVEΔVEJSed schemes at launch in 2029

Flight to Sedna using the EVEEJSed and EVEΔVEJSed schemes under the constraints (1) and (2) is significantly better in terms of ΔV_{Σ} than EJSed scheme beginning from 14 yrs TOF (Fig. 11). However, it should be emphasised that EVEEJSed and EVEΔVEJSed are significantly more complex schemes than any other ones described in this paper, which will eventually lead to higher costs for correction manoeuvres for flight using these schemes.

The catalogue of selected trajectories to Sedna using EVEEJSed and EVEΔVEJSed schemes satisfying constraints (1) and (2) is given in Appendix A, Table A.5. Fig. 12 shows the trajectory to Sedna using EVEΔVEJSed scheme for the TOF of 17-yr (Table A.5). The spacecraft trajectory parameters using the EVEΔVEJSed scheme are shown in Table 5.

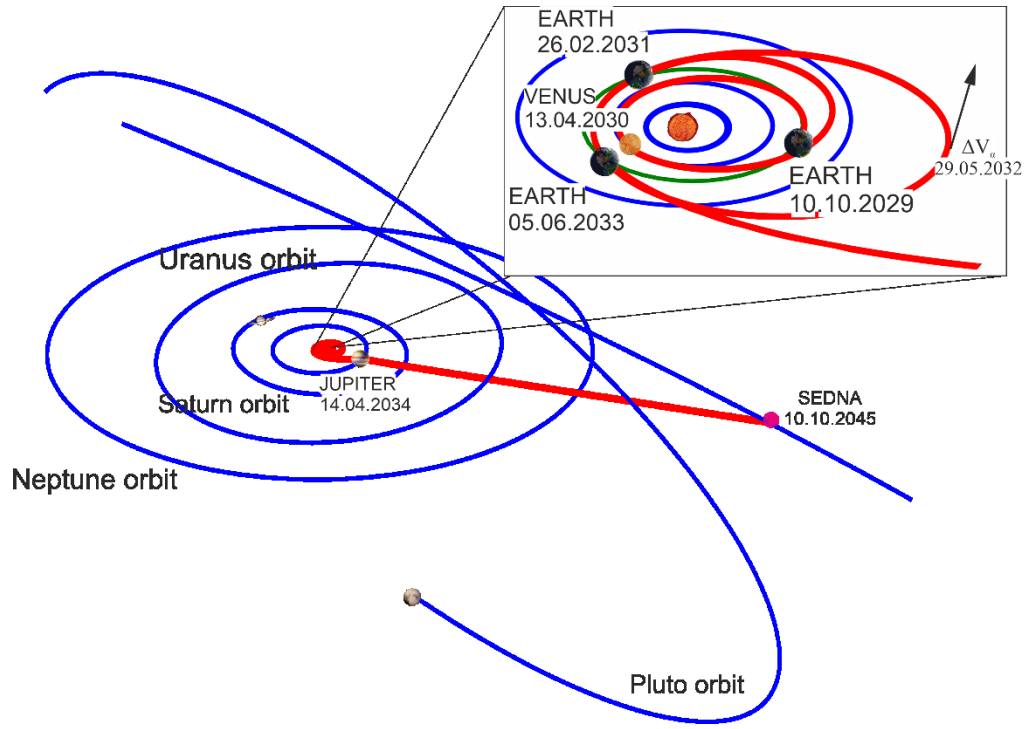


Fig. 12 Trajectory to Sedna using the EVEΔVEJSed scheme at launch in 2029

Table 5. The spacecraft trajectory parameters using EVEΔVEJSed scheme for launch at 2029 with the 17-yr TOF

Celestial bodies	Dates of Launch and flyby of celestial bodies, dd.mm.yyyy	Relative velocities near-Earth and of the flyby of celestial bodies, km/s	ΔV of launch, at aphelion and of the flyby of celestial bodies, km/s	Height of the initial orbit and flyby above celestial bodies, 10^3 km
Earth	10.10.2029	3.56	3.80	0.2
Venus	13.04.2030	5.62	0.00	7.7
Earth	26.02.2031	9.73	0.00	5.7
ΔV_α	29.05.2032	14.74	0.00	-
Earth	05.06.2033	15.80	4.54	0.3
Jupiter	14.04.2034	23.66	0.87	52.1
Sedna	10.10.2045	32.27	-	0.0*

* Approach to the object is assumed to be at any small distance

4. A flight to Sedna with the Oberth manoeuvre near the Sun

In this paper, the following scheme of the flight is considered: the spacecraft, with the help of planet gravity assists approaches the Sun at the perihelion distance from 2 to 10 Solar radii and then performs a manoeuvre required to make the value of the heliocentric velocity of the spacecraft sufficient for the flight to Sedna under the constraints (1) and (2). The optimisation problem is again to find the minimum of ΔV_Σ .

However, the main disadvantage of such scheme compared with other considered in this paper schemes is worth pointing out here. The close approach the spacecraft to the Sun would demand high-level thermal protection for spacecraft. Otherwise, a well-known example of the Parker Solar Probe mission (NASA), approaching the Sun, is supposed to be at ten solar radii (~ 7 million km) in April 2024. Despite the low pericentre height, Parker's thermal shield is only $\sim 13\%$ of its total mass³, and the shield design can significantly reduce the spacecraft's heating [31,59,60].

³ 72.9 kg out of total mass of the spacecraft ~ 555 kg [59]

In Fig. 13, a scheme of the flight to Sedna using OM is shown. The flight to Jupiter takes place at first. Then the spacecraft trajectory is reversed towards the Sun, with a subsequent OM in the vicinity of perihelion and then the spacecraft flights to Sedna.

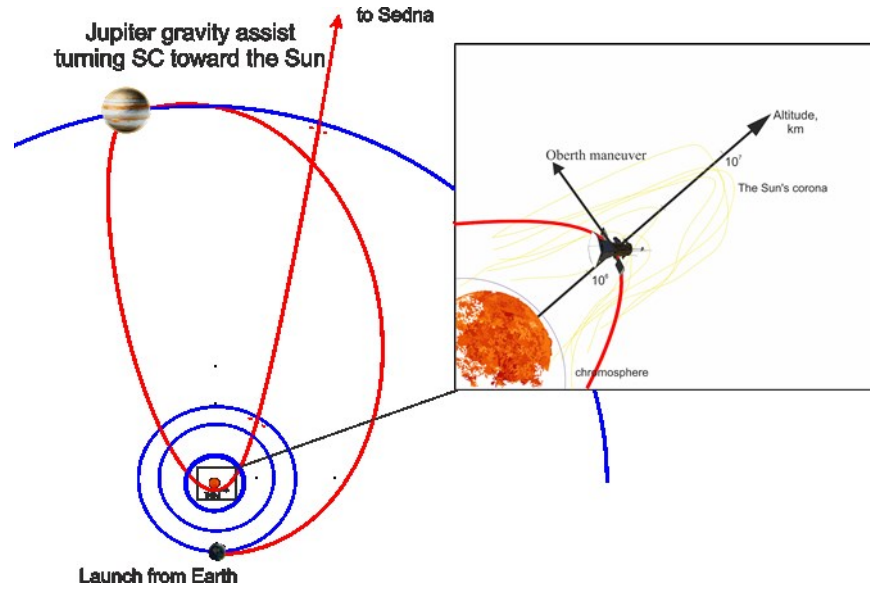
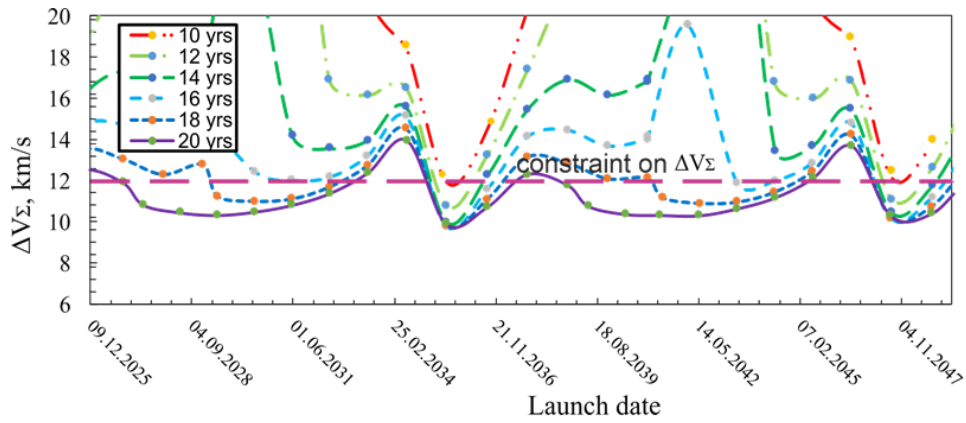
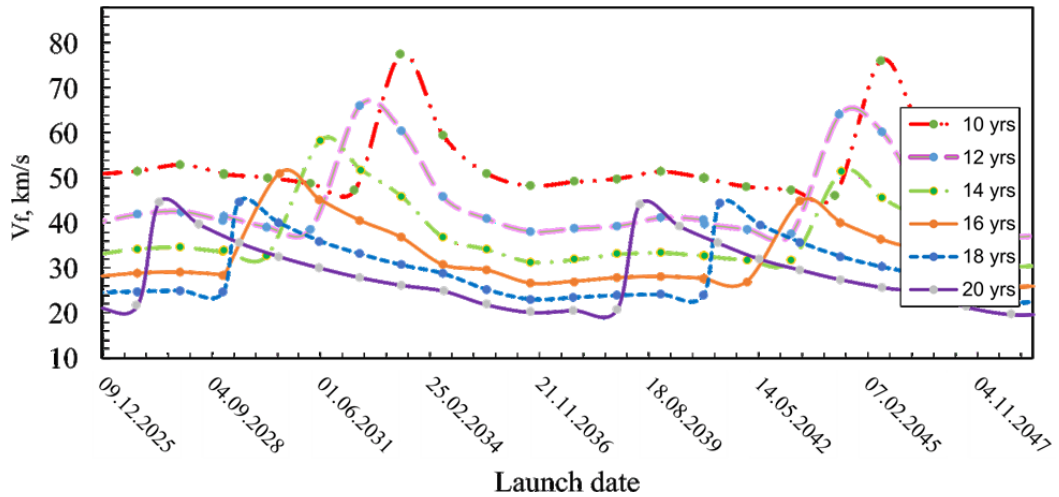


Fig. 13 Scheme of flight to Sedna with an OM near the Sun

The ΔV_{Σ} and V_f vs TOF obtained using the Earth-Jupiter-OM-Sedna (EJ-OM-Sed) scheme are plotted in Fig. 14 for a few decades. This period was chosen for the purpose of comparison EJ-OM-Sed and EJSed schemes.



(a)



(b)

Fig. 14 (a) ΔV_{Σ} for 10; 12; 14; 16;18 and 20-yr TOF vs. launch dates, (b) V_f curves for 10; 12; 14; 16;18 and 20-yr TOF vs launch dates.

Notice, the flight using the EJ-OM-Sed scheme (Fig. 14.a) is almost opposite to the one using the EJSed scheme (Fig. 2.a). From the other hand the flight using EJ-OM-Sed requires higher ΔV_{Σ} than using EJSed scheme. Let us compare the best launch dates for the flight using EJSed in 2032 (Fig 2.a) and EJ-OM-Sed in 2035 (Fig. 14.a).

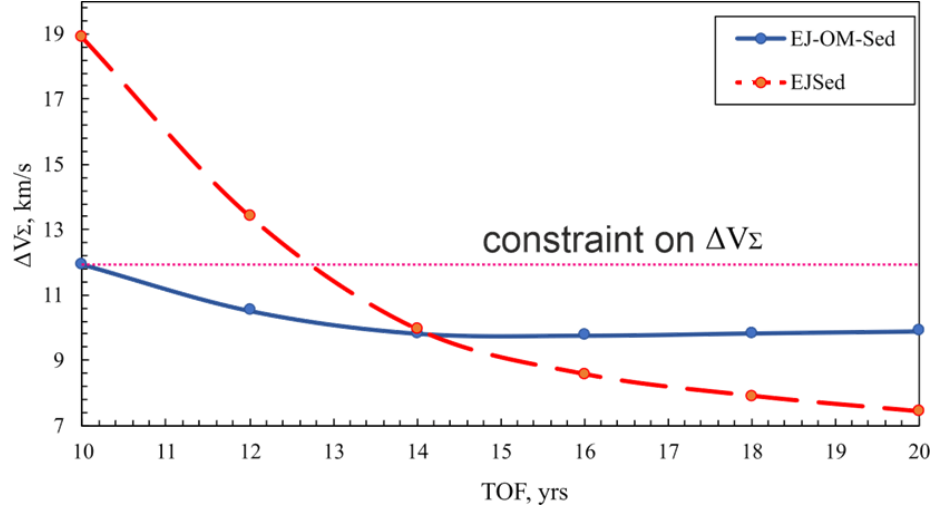


Fig. 15 Comparison of EJSed and EJ-OM-Sed schemes by ΔV_{Σ} for the best launch dates in 2032 and 2035, respectively

The application of such a scheme with OM (i.e. EJ-OM-Sed in Fig. 15) gives the greatest benefit for a TOF less than 14-yr (Table 6) compared with the other mentioned in this paper schemes. However, since ΔV_{Σ} using the scheme is always greater than 9.8 km/s for any launch date out of the period under consideration, the scheme does not seem appropriate for the TOF of 15-yr or more.

As it was mentioned above, the requirement of ensuring the extra thermal shield of the spacecraft reduces its final mass by about 15% that is the main disadvantage of the used scheme. However, it should be emphasised that the flight was considered only with the high thrust, but the situation might completely change in the case of using the low thrust. For the low thrust, such proximity (Table 6) to the Sun may be an advantage, as it allows the use of promising technology, namely a solar sail. As it was shown in studies [30,31,39,42,61], the application of such technology will enable the spacecraft to accelerate up to 20-25 AU/y (94.8-118.5 km/s) manoeuvring near the Sun, while the best result obtained with the high thrust is only 8-11 AU/y (37.9-52.1 km/s) at a very close approach to the Sun and the ΔV manoeuvre value of ~3-4 km/s. Increasing the final velocity to 20-25 AU/y would require an impulse of at least 8 km/s, which is impractical for our target.

Table 6. Catalogue of selected trajectories to Sedna by EJ-OM-Sed scheme satisfying constraints (1) and (2)

Optimal launch date, dd.mm.yyyy	TOF, yrs	Jupiter flyby date, dd.mm.yyyy	Height of Jupiter flyby, 10 ³ km	ΔV_{Σ} , km/s	V_f , km/s	$r_{\text{sun,*}}$ 10 ⁶ km
15.05.2029	18	07.02.2037	951.1	11.24	44.83	2.3
11.05.2029	20	28.12.2036	859.2	10.32	35.75	2.4
16.05.2030	18	14.01.2037	973.7	11.00	40.04	2.3
15.05.2030	20	09.01.2037	966.5	10.49	32.64	2.6
22.05.2031	16	06.02.2037	1,220.0	12.00	45.31	2.3
18.05.2031	18	24.12.2036	1,089.3	11.10	36.12	2.5
19.05.2031	20	10.01.2037	1,109.9	10.80	30.04	3.5
24.05.2032	16	16.01.2037	1,521.7	12.15	40.52	2.3
24.05.2032	18	19.01.2037	1,480.9	11.67	33.10	3.1
26.05.2032	20	07.02.2037	1,446.2	11.37	27.97	4.7
24.07.2035	10	06.10.2036	178.4	11.95	51.35	2.3
23.07.2035	12	20.10.2036	308.8	10.53	41.21	2.3
23.07.2035	14	30.10.2036	437.9	9.83	34.22	2.3
22.07.2035	16	11.11.2036	390.0	9.77	29.53	2.4

22.07.2035	17	30.11.2036	404.4	9.84	25.23	3.1
21.07.2035	19	14.12.2036	423.9	9.90	21.96	3.7
29.08.2036	14	17.10.2037	3.7	12.25	31.41	11.1
29.08.2036	16	18.10.2037	3.6	11.58	26.59	13.0
29.08.2036	18	23.10.2037	7.3	11.09	23.02	15.1
29.08.2036	20	31.10.2037	16.3	10.72	20.27	17.1
28.10.2038	20	24.11.2040	3.6	11.78	20.94	2.3
28.11.2039	20	28.01.2042	3.6	11.01	21.13	2.3
24.05.2040	18	18.04.2049	975.2	11.81	50.35	2.3
20.05.2040	20	17.03.2049	839.7	10.36	39.30	2.3

**perihelion distance of the spacecraft*

Table 7 shows the spacecraft trajectory parameters of the flight to Sedna, using the EJ-OM-Sed scheme, at launch in 2035. Fig. 16 shows the trajectory of the corresponding flight.

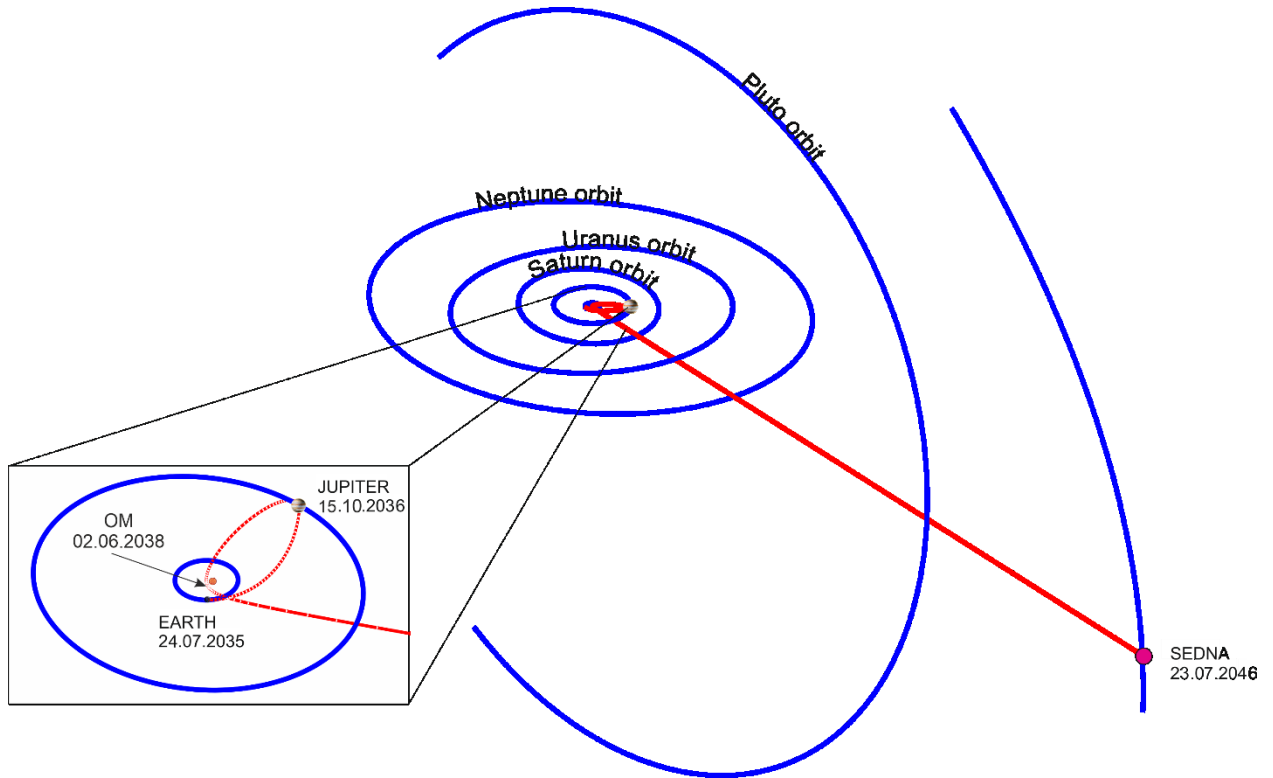


Fig. 16 Trajectory of spacecraft flight to Sedna for the launch in 2032 using EJ-OM-Sed scheme

Table 7. The spacecraft trajectory parameters using EJ-OM-Sed scheme with 11-yr TOF for launch in 2035

Celestial bodies	Dates of Launch and flyby of celestial bodies, dd.mm.yyyy	Relative velocities near-Earth and of the flyby of celestial bodies, km/s	ΔV of launch, at aphelion and of the flyby of celestial bodies, km/s	Height of the initial orbit and flyby above celestial bodies, 10^3 km
Earth	24.07.2035	11.24	7.94	0.2
Jupiter	15.10.2036	13.93	0	244.5
OM (Sun)	02.06.2038	367.00	3.17	2,000.0
Sedna	23.07.2046	45.79	-	0.0*

* Approach to the object is assumed to be at any small distance

As shown in Table 7, while approaching the Sun the spacecraft accelerates to the 367 km/s, and while approaching Sedna its velocity V_f is about 45.79 km/s which is higher than in all other schemes (Table 1-5). Considering this value, the flyby Sedna would be fast, resulting in blurring images taken by on-board cameras.

5. Estimation of the spacecraft's mass delivered to Sedna

The final mass of the spacecraft delivered to Sedna was estimated using the rocket equation [62]. For this estimation, we used the launch vehicles presented in Table 8.

Table 8. Characteristics of analysed launch vehicles

Rocket	Mass in the Low Earth Orbit, 10^3 kg	Fuel capacity, 10^3 kg	Dry mass of the last stage, 10^3 kg	The specific impulse of the last stage, s
Soyuz 2.1.b / Fregat * (fourth stage)	8.2	~5.6	0.97	333.2
Proton-M / DM-03** (fourth stage)	23.7	~18.0	2.34	355
Delta IV Heavy***, 1/DCSS (second stage)	28.8	27.2	3.48	462
Space Launch System (SLS)***, 1/ICPS (second stage)	95.0	27.2	3.50	465.5

* - performance is given under the condition of launch from Vostochny site

** - performance is given under the condition of launch from Baikonur site

*** - performance is given under the condition of launch from Cape Canaveral (airforce base) site

¹ – performance curves obtained in works [63] and through launch calculator by <https://elvperf.ksc.nasa.gov/Pages/Default.aspx>

It should be noted that it is assumed that a chemical upper stage is used for performing manoeuvres on the interplanetary arcs in all cases. The analysed upper stage has a specific impulse of 308 s, which is provided by using two components fuel: asymmetrical dimethylhydrazine (fuel) and nitrogen tetroxide (oxidiser). The constant mass of the upper stage is 110 kg. The mass of the tanks is calculated in 15% out of the fuel mass.

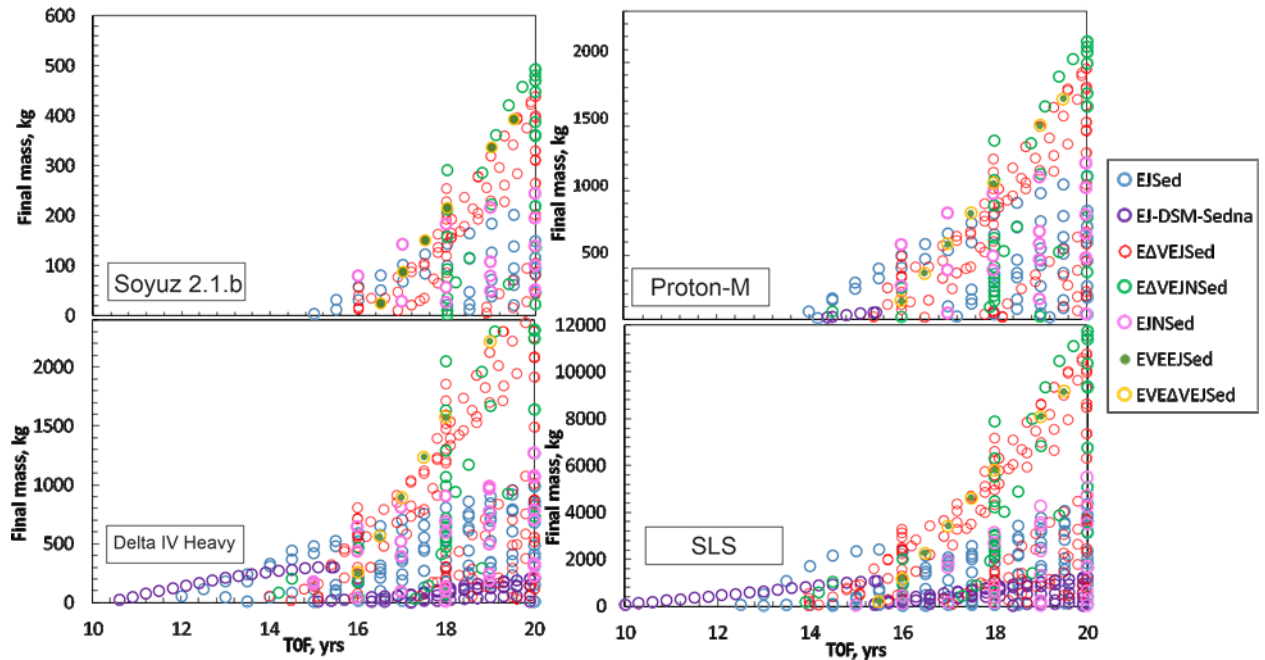


Fig. 17 The final mass brought to Sedna vs TOF for every considered scheme and considered launch vehicles

The distribution of the final mass in Fig. 17, depending on the used scheme and the used launch vehicle, demonstrates the technical possibility of a flight to Sedna under conditions (1) and (2). Using a middle-class launch vehicle (Soyuz 2.1.b), the payload mass delivered to Sedna would be up to 550 kg for a 20-year TOF. This value is twice more than for Pioneer 10, Pioneer 11 and is a half of the mass of Voyager 1, Voyager 2. However, using the super-heavy class, it is possible to deliver to Sedna up to 12,000 kg of the payload, which makes an orbiting Sedna theoretically possible. However, due to the high flyby velocity of the spacecraft, this payload mass still might not be enough to produce a braking impulse comparable to the flyby velocity (>20 km/s).

6. Remark on the close Jupiter flyby

Almost all the schemes used in the research require the close flyby of Jupiter at a distance of less than 1 million km. In such a case, the spacecraft might be exposed due to an intense radiation load. The authors of the research [64], based on the dipole approximation of the magnetic field model of Jupiter ('O4' model by [65]), estimated the vehicle radiation exposure during the Jupiter flyby. According to the results obtained, a Jupiter flyby without causing damage of an on-board equipment is possible if the flight altitude and inclination are greater than 136 thousand km and 40 degrees [64], respectively. Later studies [66] show that a safe passage at any inclination of the spacecraft orbit is possible at an altitude over 600 thousand km (8.4 radii of Jupiter).

The analysis prepared in this paper was conducted using free SPENVIS software⁴ for the Divine & Garret radiation model [67] at an average trajectory inclination of 25 degrees to the Jupiter equatorial plane. The simulation results for the aluminium shielding are shown in Fig 18. It is shown that a Jupiter flyby is possible only if the permanent radiation shielding of the spacecraft is increased by at least 10-20 mm. In that case, radiation will be about 100-200 krad which is close to the Galileo exposure ~290 krad. Note that this thickening of the shielding leads to an increase in mission cost and a reduction in payload mass.

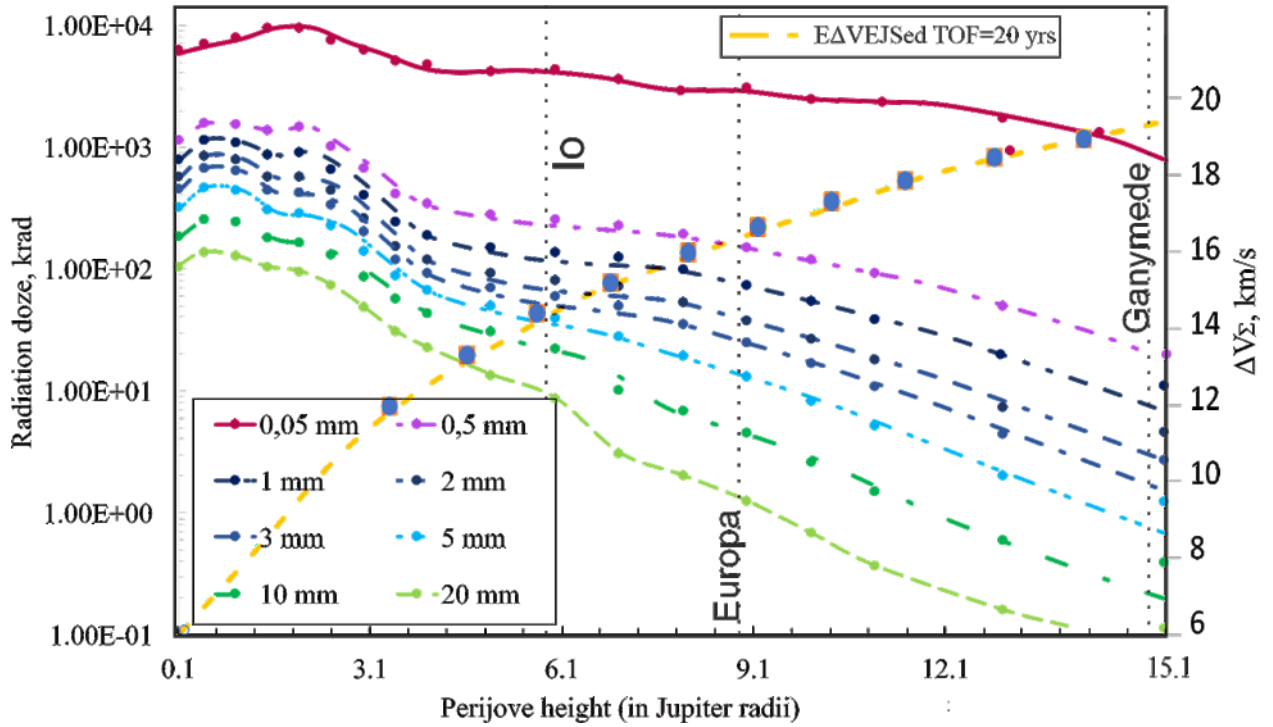


Fig. 18 Total radiation dose and ΔV_{Σ} cost vs perijove height

The height of the Jupiter flyby can be raised to any desired value, but this inevitably would lead to increasing ΔV costs. For example, Fig. 18 shows an estimate for the increase in total ΔV_{Σ} vs perijove height during a flight according to the EAVEJSed scheme. This Fig. 18 shows that the increasing flyby pericenter altitude to the height of Ganymede orbit would be accompanied with an over 3-fold increase in ΔV_{Σ} . Taking this into account, the best solution, in this case, would be to increase the shielding thickness of the spacecraft and flyby at a low altitude near Jupiter than to increase the flyby altitude of the spacecraft.

7. The best flight schemes to Sedna

Above in this paper, schemes of flight to Sedna fulfilling restrictions (2) and (3) were considered. However, it should be noted that a flight under constraint (3) represents a relatively complicated technical task or may require the use of heavy or super-heavy launch vehicle. Therefore, it is reasonable to select a less energy expansive scheme, i.e. to decrease the constraint (3) down to ~9 km/s that is similar to the ΔV used in New Horizons⁵ mission [25,27,58]. Table 9 shows a catalogue of such schemes. Mass estimates are given only for medium and heavy launch vehicles (Soyuz 2.1.b, Proton-M) since the ΔV_{Σ} limit allows the use of less expensive launch vehicles than super-heavy ones (such as Space Launch System (SLS)).

⁴ SPENVIS software web page: <https://www.spenvis.oma.be/models.php> (Accessed 20 September, 2021)

⁵ New Horizons mission web-page URL: https://www.nasa.gov/mission_pages/newhorizons/main/index.htmls

Table 9. Catalogue of the best schemes of flight to Sedna based on ΔV_{Σ}

Scheme	Launch date, dd.mm.yyyy	TOF, yrs	ΔV_{Σ} , km/s	Final mass delivered to Sedna		V_f , km/s
				Soyuz 2.1.b, 10^3 kg	Proton-M, 10^3 kg	
EJSed	31.03.2032	20	7.42	0.22	1.07	19.73
EJNSed	04.04.2044	20	7.29	0.24	1.15	20.34
E Δ VEJSed	02.03.2029	20	6.36	0.44	1.87	23.91
E Δ VEJNSed	08.03.2041	20	6.13	0.49	2.07	24.59
EVVEJSed & EVE Δ VEJSed	08.11.2029	20	6.27	0.47	1.90	23.60

The scheme with OM near the Sun does not satisfy constraint by 9 km/s but provides a flight to Sedna with 10-14 yrs duration satisfying the constraint (2). That is the primary reason why this scheme is considered in Table 10. Note, for the EJ-OM-Sed scheme in Table 10, the mass would be considered only for heavy and super-heavy launch vehicles (Delta IV Heavy, Space Launch System (SLS)). Results for other schemes are given in Table 10 considering the ~ 9 km/s limits.

Table 10. The fastest routes to Sedna

Scheme	Launch date, dd.mm.yyyy	TOF, yrs	ΔV_{Σ} , km/s	Final mass delivered to Sedna, 10^3 kg	V_f , km/s
EJSed	29.03.2032	15.1	9.02	0.30 (Proton-M)	27.49
EJNSed	10.04.2044	15.7	9.07	0.29 (Proton-M)	26.67
E Δ VEJSed	24.02.2042	16.0	8.95	0.31 (Proton-M)	29.96
E Δ VEJNSed	09.05.2041	18.0	8.99	0.31 (Proton-M)	27.90
EVVEJSed & EVE Δ VEJSed	02.11.2029	16.2	9.05	0.22 (Proton-M)	31.60
EJ-OM-Sed	24.07.2035	10.0	11.95	0.10 (SLS)	51.35

The best scheme providing the smallest value of ΔV_{Σ} under constraint (2) is the E Δ VEJNSed scheme enabling $\Delta V_{\Sigma}=6.13$ km/s for the TOF of 20-yr at launch in 2041 (Table 9). Note that due to the gravity assist of Neptune, there are no earlier launch windows ensuring $\Delta V_{\Sigma}=6.13$ km/s than in 2041. The next available launch window will be in 2054, after which the ΔV_{Σ} for TOF of 20-yr will steadily increase. Therefore, for a launch before 2041, the EVE Δ VEJSed (EVVEJSed) scheme for a launch date in 2029 appears most appropriate, since in that case, a 20-year flight would require $\Delta V_{\Sigma}=6.27$ km/s (Table 9). The trajectories of the spacecraft flight using E Δ VEJNSed and EVE Δ VEJSed schemes are given in Fig 8 and Fig 12.

If reaching Sedna in the shortest time while satisfying constraint (1) is needed, it is better to use the EJ-OM-Sed scheme, as TOF of 10-yrs is possible with this scheme. If the constraint (1) needs to be reduced to 9 km/s, using EJSed is best since it takes 15.1 years to reach Sedna (Table 10). The trajectories of the spacecraft flight using EJSed and EJ-OM-Sed schemes are given in Fig 3 and Fig 16.

8. Possible expansion of space mission to Sedna

The global practice of maximising the scientific output through expanding the research program of space missions is well known. For example, during the NEAR [68,69] mission to the asteroid (433) Eros, it also approached the asteroid (253) Matilda, making it possible to determine its mass and obtain photos of its surface. There are also known examples of Galileo [70] (approaching (243) Ida and (951) Gaspra), Cassini–Huygens ((2685) Masursky) [71], Ulysses (passing the gas tail of a few comets), and New Horizons [72] (TNO (486958) Arrokot flyby) missions, etc. Taking as an example the mentioned missions, we carry out a study of possible expansion of the flight scenario to Sedna.

One way of expanding the mission to Sedna may be to explore the planets and their satellites during gravity assist manoeuvres. Another way of expanding the mission scenario could be provided by including close encounters of small celestial bodies. In the paper [43], the main belt asteroids that could be encountered during the flight to Sedna

were considered as potential additional targets. This paper proposes a different way of expansion: sending a small spacecraft to another TNO during the primary flight to Sedna. For that purpose, it is proposed that the spacecraft should consist of two modules: a vehicle to study Sedna and a small space probe, which would be separated from the main spacecraft during the last gravity assist manoeuvre and then directed to another TNO. Note that similar research of study two objects in one mission with spacecraft separation was proposed in articles [23,61] for studying classical KBOs.

The general optimization scheme considered above will not be significantly changed. However, there is a specific feature of the algorithm used in this section. Like in the previous case, the model of patched conic approximation is used. Impulses needed during the gravity assist are described in sec. 3.1. The new one added in this section is required for a separation of the probe from the main spacecraft and directing it to another TNO (ΔV_s). The ΔV_s value was calculated using the method described in [65]. Note that for implementation of the method the separation of spacecrafts is considered to be on the SOI boundary of the last flyby planet.

Let us limit the magnitude of the separation impulse as follows:

$$\Delta V_s \leq 300 \text{ m/s} \quad (3)$$

No restrictions are imposed on the TOF to the second chosen TNO. It is assumed that the flight to another TNO is unpowered, i.e. without any additional manoeuvres. Nevertheless, the used optimisation process considers the manoeuvres of the probe inside the SOI. Hence all probe trajectory required powered gravity assist were removed in the final selection process.

A total of 5 suitable trans-Neptunian bodies were selected (Table 11), namely three extreme TNOs (2012 VP₁₁₃ ('Biden'), Leleākūhonua (former 2015 TG₃₈₇), 2013 SY₉₉) and two classical Edgeworth-Kuiper belt objects: (90482) Orcus and (20000) Varuna. The results for all flights satisfying constraints (1), (2) and (3) are presented in Table 12.

Table 11. Parameters of Sedna and the TNOs suitable for proposed mission expansion

TNO	d*, km	Orbital elements**						T, yrs
		q, AU	a, AU	e	i, deg	Ω, deg	ω, deg	
Sedna [8]	~1000	76.341	499.469	0.847	11.931	144.208	311.130	11,162.77
2012 VP ₁₁₃ [21]	~600	80.412	266.462	0.698	24.089	90.720	293.659	4,349.73
Leleākūhonua [4]	~300	65.172	1,210.470	0.946	11.655	300.795	117.648	42,115.24
2013 SY ₉₉ [73]	~250	50.080	792.110	0.936	4.216	29.526	31.718	22,293.92
Orcus [7]	761...917	30.155	39.110	0.228	20.584	268.725	72.701	244.60
Varuna [74,75]	859×453	40.265	42.724	0.057	17.209	97.350	263.222	279.27

* d is TNOs diameter, calculated assuming albedo taken in <https://ssd.jpl.nasa.gov/sbdb.cgi#top>; **Orbital elements are given w.r.t. to Ecliptic plane J2000 Epoch; Designation used in the table: q is the perihelion distance, a is the semi-major axis, i is the inclination, e is the eccentricity, Ω is the longitude of ascending node, ω is the argument of pericentre, T is the orbital period.

Table 12. Catalogue of selected schemes providing exploration of both Sedna and another TNO simultaneously

Target TNOs	Scheme	Launch date, dd.mm.yyyy	TOF, yrs	ΔV_s , km/s	Date of separation, dd.mm.yyyy	Pericentre height*, 10 ³ km	TOF ₁ **, yrs	ΔV_s ***, km/s	V_e ****, km/s
2012 VP ₁₁₃	EJSed	01.04.2032	18	7.90	24.06.2033	55.0	19.8	0.020	19.91
		31.03.2032	20	7.42	24.07.2033	101.8	21.8	0.023	17.97
		10.05.2033	18	8.22	27.06.2034	429.4	21.2	0.039	18.04
		09.05.2033	20	7.87	21.07.2034	617.5	24.8	0.052	15.27
		22.06.2034	18	9.82	31.05.2035	1421.2	23.1	0.167	16.24
		20.06.2034	20	9.37	15.06.2035	1926.8	27.0	0.225	13.72
		26.01.2039	20	9.87	13.08.2045	3.6	30.7	0.034	12.81
	EJNSed	19.12.2040	20	8.63	11.08.2043	43.6	14.1	0.012	20.82
		19.01.2041	20	7.94	23.01.2045	51.0	13.4	0.014	21.87
		28.02.2043	18	8.86	22.02.2045	52.6	13.5	0.015	21.76
		28.02.2043	20	7.58	09.02.2045	87.8	15.6	0.019	18.73
		06.04.2044	18	7.65	07.07.2045	69.7	14.4	0.017	20.25
		04.04.2044	20	7.29	12.08.2045	110.6	16.6	0.022	17.56
	EAVEJSed	27.02.2029	18	7.68	18.09.2033	244.9	26.5	0.01	14.45

Leleākūhonua	EΔVEJNSed	02.03.2029	20	6.36	29.06.2033	56.2	19.8	0.01	19.90
		15.04.2030	18	8.07	04.06.2034	282.5	18.3	0.01	21.15
		13.04.2030	20	6.92	17.06.2034	340.7	19.5	0.01	19.75
		03.05.2040	20	6.31	11.05.2045	40.82	10.6	0.013	23.41
		09.05.2041	18	8.99	20.05.2045	29.06	12.5	0.01	25.36
		05.05.2041	20	6.18	12.05.2045	54.84	11.6	0.015	21.67
		17.06.2042	18	9.08	11.06.2045	35.58	13.5	0.012	24.08
		13.06.2042	20	7.38	29.04.2046	62.28	12.2	0.016	20.58
	EJSed	01.04.2032	18	7.90	25.06.2033	757.0	19.5	0.176	16.03
		31.03.2032	20	7.42	24.07.2033	1163.1	24.9	0.23	12.07
		05.04.2044	18	7.85	22.07.2045	759.8	20.0	0.172	14.73
		05.04.2044	20	7.39	01.08.2045	867.3	21.4	0.18	13.58
	EΔVEJSed	27.02.2029	18	7.68	18.09.2033	1867.3	50.9	0.300	5.1
		03.03.2029	20	6.36	29.06.2033	753.5	19.5	0.200	16.0
		16.01.2038	20	9.10	09.09.2045	3.6	68.6	0.100	3.7
2013 SY ₉₉	EJSed	27.01.2030	18	8.90	16.04.2033	39.1	49.0	0.060	3.82
		01.04.2032	18	7.90	24.06.2033	271.3	11.1	0.085	20.81
		31.03.2032	20	7.42	24.07.2033	399.2	12.5	0.095	18.28
		10.05.2033	18	8.22	27.06.2034	1,419.8	14.8	0.274	14.46
		05.04.2044	18	7.85	21.07.2045	169.2	11.3	0.070	19.70
		04.04.2044	20	7.39	01.08.2045	195.2	11.6	0.072	18.97
	EΔVEJSed	07.05.2030	18.0	7.31	01.08.2033	455.2	13.1	0.119	17.23
		07.05.2030	20.0	6.70	25.07.2033	417.3	12.7	0.106	17.82
		14.06.2031	20.0	7.17	24.06.2034	1,411.9	14.9	0.271	14.32
		06.03.2040	20.0	7.77	01.09.2044	119.6	43.8	0.056	4.04
		11.04.2041	20.0	8.72	03.10.2045	195.9	58.0	0.073	3.16
		10.05.2042	18.0	7.26	11.10.2045	491.6	15.4	0.127	13.62
		20.06.2043	18.0	7.61	09.06.2046	521.1	10.7	0.099	19.91
		18.06.2043	20.0	6.99	09.07.2046	788.0	12.8	0.129	16.33
	EΔVEJNSed	21.09.2041	20	9.21	11.05.2051	136.5	4.5	0.037	21.30
		14.05.2042	18	7.19	01.12.2050	108.4	4.1	0.034	23.71
		12.05.2042	20	6.47	11.09.2051	145.6	4.7	0.038	20.56
		21.06.2043	18	8.22	07.09.2051	114.6	4.3	0.034	22.62
		20.06.2043	20	7.58	01.06.2052	152.4	4.9	0.038	19.62
	EJNSed	19.12.2040	20	8.63	12.06.2050	127.1	4.6	0.035	21.19
		19.01.2041	20	7.94	21.01.2051	124.9	4.3	0.036	22.26
Orcus	EΔVEJSed	05.06.2029	18	9.06	06.07.2034	3.6	25.5	0.100	7.68
		25.02.2029	20	7.21	07.10.2033	3.6	38.0	0.100	4.27
		18.02.2030	18	7.33	14.10.2033	3.6	40.6	0.100	3.90
		10.04.2030	20	7.23	16.07.2034	3.6	25.7	0.100	7.63
		05.04.2031	20	7.40	15.07.2034	3.6	25.8	0.100	7.60
Varuna	EJSed	31.03.2032	18	7.92	14.07.2033	3.6	25.1	0.069	7.11
		31.03.2032	20	7.42	24.07.2033	10.9	26.5	0.078	6.60
		10.05.2033	18	8.22	27.06.2034	79.4	23.6	0.132	7.93
		08.05.2033	20	7.87	21.07.2034	92.7	23.1	0.142	8.06
		22.06.2034	18	9.82	31.05.2035	108.3	55.4	0.238	4.20
		20.06.2034	20	9.37	15.06.2035	131.8	55.1	0.269	4.01
		03.02.2038	20	9.82	26.12.2045	1,087.2	36.4	0.22	4.34
		06.02.2039	20	9.16	04.01.2046	1,166.7	39.7	0.223	3.87
		07.02.2040	18	9.80	01.12.2045	1,418.7	46.3	0.247	3.19
	EΔVEJSed	09.02.2040	20	8.66	03.01.2046	1,319.2	45.2	0.234	3.30
		05.06.2029	18	8.25	24.04.2034	43.2	23.9	0.100	8.14
		16.04.2029	20	7.08	10.06.2034	67.6	24.6	0.100	7.67
		09.06.2030	18	7.83	06.05.2034	49.5	23.9	0.100	8.08
		13.04.2030	20	6.92	17.06.2034	72.3	24.4	0.100	7.70

* Height of the pericentre calculated for the probe trajectories after the probe separation

** TOF₁ is the time of flight after the probe separation to the TNO;

*** ΔV_s is the separation impulse at a distance of 80 mln. km from the flyby planet;

**** V_e is the flyby velocity near the second TNO.

For example, the flight to Sedna and the sednoid 2012 VP₁₁₃ ('Biden') using the EΔVEJSed scheme with the launch on 02.03.2029 and TOF (to Sedna) equal to 20-yr is considered. The orbital diagram is shown in Fig. 19; the corresponding spacecraft's trajectory parameters are shown in Table 13.

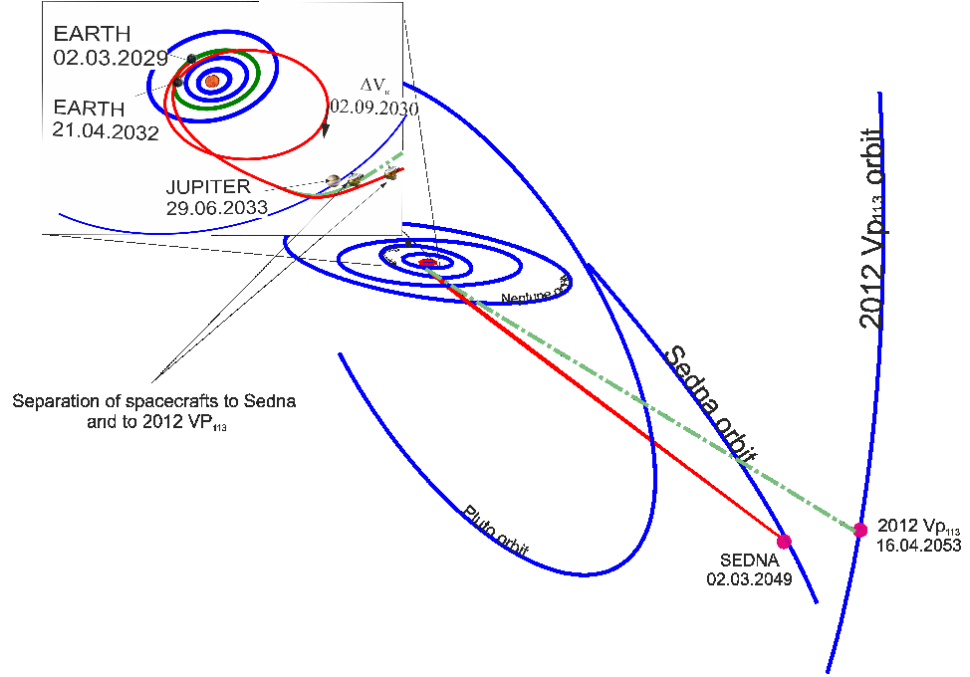


Fig. 19 Trajectory of spacecraft and probe flight to Sedna and 2012 VP₁₁₃ for launch on 02.03.2029 using EΔVEJSed scheme

Table 13. The spacecraft and probe trajectory parameters to Sedna and 2012 VP₁₁₃ using EΔVEJSed scheme for launch on 02.03.2029

Celestial bodies/deep space manoeuvres	Dates of launch and flyby of celestial bodies, dd.mm.yyyy	Relative velocities near-Earth and of the flyby of celestial bodies, km/s	ΔV of launch, at aphelion and of the flyby of celestial bodies, km/s	Height of the initial orbit and flyby above celestial bodies, 10 ³ km
Earth	02.03.2029	7.02	5.28	0.2
ΔV _α	02.09.2030	10.64	0.60	-
Earth	21.04.2032	12.36	0.00	0.3
Jupiter (to Sedna)	29.06.2033	16.46*	0.48	3.7
Jupiter (to 2012 VP ₁₁₃)	29.06.2033	16.46*	0	56.3
Sedna (the spacecraft)	02.03.2049	22.44	-	0.0**
2012 VP ₁₁₃ (the probe)	16.04.2053	19.88	-	0.0**

* The value of incoming relative velocity is given.

**Approach to the object is assumed to be at any small distance

9. Conclusions

In this paper, the flight schemes to Sedna, providing its fast approach for studying the object at the closest possible distance were analyzed. Both the direct flight scheme to the object and schemes including a series of gravity assists of planets were considered. It is demonstrated that a flight to Sedna can be performed almost each year beginning from 2029 under a constraint on the TOF (constraint (1)) with the ΔV_Σ limit up to 12 km/s (constraint (2)). Moreover, the ΔV_Σ limit (2) can be easily reduced to ~9 km/s.

The direct flight to Sedna can be performed each year because of the synodic period of Earth and Sedna. Flight with considered constraint on TOF of 20-yr requires launch ΔV of at least

14 km/s. Thus, a direct flight to Sedna is hardly possible with the existing technical means because the flight with duration of 20 years or less would require usage of super heavy launch vehicles.

The best of the EJSed, EJNSed, EΔVEJSed, EΔVEJNSed, EVEΔVEJSed (EVEEJSed), EJ-OM-Sed flight schemes proved to be the EΔVEJNSed scheme for TOF=20-yr, providing the minimum $\Delta V_{\Sigma} = 6.13$ km/s. In that case, 490 kg can be delivered by a light class Soyuz 2.1.b rocket and 2,070 kg by a medium-class Proton-M rocket. If the main criterion of choosing the flight scheme is to reach Sedna as soon as possible, and the ΔV_{Σ} limit (1) must be met, the EJ-OM-Sed scheme is best, allowing a ~100 kg payload mass delivery to Sedna by the SLS. However, this scheme would require a close approach to the Sun of up to 2 solar radii, so using the classic and well known EJSed scheme seems most appropriate. It takes 15.1 years to reach Sedna at the cost of $\Delta V_{\Sigma} = 9.01$ km/s using the EJSed scheme, and a 295.5 kg payload would be delivered to Sedna by Proton-M in this case.

The estimation of the final mass of the spacecraft delivered to Sedna shows that the results of ΔV_{Σ} for the schemes considered in the paper allow to easily obtain from 50 to 12,000 kg on the flyby trajectory near Sedna depending on the launch vehicle used. The maximum payload mass for all investigated schemes is achieved at TOF=20-yr. B, Proton-M, Delta-IV Heavy and SLS, respectively. For the EJSed and EJNSed schemes the maximum payloads using Soyuz 2.1.b and Proton-M rockets will be ~300 kg and ~1,200 kg while using Delta-IV Heavy and SLS to Sedna provides ~1,300 kg and ~4,500 kg respectively. The ΔVEGA manoeuvre schemes (EΔVEJSed, EΔVEJNSed and EVEΔVEJSed (EVEEJSed)) using Soyuz 2.1 can deliver maximum 500 kg, 2000 kg, 2,000 kg and 12,000 kg. The EJ-OM-Sed scheme would achieve the maximum payload mass of about 300 kg and 1,000 kg using Delta IV Heavy and SLS rockets.

As a potential expansion of the mission to Sedna, the scenario of a two-target mission was considered. One of the targets of this mission is Sedna, and the others are the TNOs that can be reached without an additional increase of ΔV_{Σ} . Five TNOs have been found to which a flight under such conditions is possible. Three of these objects are extreme TNOs (2012 VP₁₁₃, 2013 SY99, Leleākūhonua) with an orbital period of about 4, 22 and 44 thousand years correspondingly. The others are classic KBOs: Orcus and Varuna. The best results were obtained for 2012 VP₁₁₃, as passive flight is achieved by almost any of the schemes considered (see Table 12).

Summarising all of the above, we would like to emphasize that despite the distance of Sedna from the Earth, at the current level of rocket and space technology, there are hardly technical difficulties in exploring Sedna even from the aspect of flyby trajectory. Yet the exploration of such an object could be the first step for mankind to interstellar space.

Acknowledgments

The author is sincerely grateful to Dr Alexander Sukhanov and Dr Konstantin Fedyaev, leading mathematicians of the Space Research Institute of the Russian Academy of Sciences, and Dr Natan Eismont, the leading researcher of the Space Research Institute of the Russian Academy of Sciences, Dr Vsevolod Koryanov and to my colleague Andrey Belyaev for their essential help during the paper's preparation and their help with the English translation and proof-reading.

Also, author want to sincerely thank the participants of the Seminar on mechanics, control and informatics dedicated to optimal flight to Sedna⁶. The meeting led by Prof. R.R. Nazirov was held in the Space Research Institute (IKI) of the Russian Academy of Sciences. The seminar participants' comments helped to improve obtained results, which subsequently was included in this paper.

Appendix A

In this appendix, the trajectory catalogues for the flight schemes to Sedna discussed in this paper are compiled. Tables A.1-A.2 and A.5 contain data for the flight schemes without a gravity manoeuvre near Neptune. The catalogues are built for launch dates from 2029 to 2042, i.e. for one orbital period of Jupiter. Tables A.3 and A.4 are derived for schemes with gravity assist of Neptune for launch dates after 2039. The trajectories in all the below tables satisfy constraints (1) and (2) simultaneously.

Table A.1. Catalogue of selected trajectories to Sedna by the EJSed scheme

Optimal launch date, dd.mm.yyyy	Launch window*, dd.mm	TOF, yrs	Jupiter flyby date, dd.mm.yyyy	Height of Jupiter flyby, 10 ³ km	ΔV_{Σ} , km/s	V_f , km/s
---------------------------------------	-----------------------------	-------------	--------------------------------------	---	-------------------------------	-----------------

⁶ The Seminar's web page http://iki.rssi.ru/seminar/20210611/e_abstract.php

28.01.2029	25.01-05.02	16	25.07.2033	3.6	10.77	33.01
31.01.2029	24.01-09.02	18	19.09.2033	3.6	9.25	28.08
03.02.2029	23.01-11.02	20	21.10.2033	3.6	8.34	24.31
27.01.2030	17.01-05.02	16	18.03.2033	3.6	10.56	29.72
27.01.2030	16.01-05.02	18	16.04.2033	3.6	8.90	25.60
01.02.2030	22.01-03.02	20	09.07.2033	3.6	8.10	22.51
17.02.2031	08.02-25.02	18	16.10.2033	3.6	10.55	24.24
16.02.2031	07.02-26.02	20	09.10.2033	3.6	9.40	21.25
30.03.2032	08.02-26.02	14	14.12.2033	3.6	9.95	30.42
31.03.2032	20.03-10.04	16	28.07.2033	3.6	8.57	25.57
01.04.2032	21.03-11.04	18	25.06.2033	14.1	7.90	22.24
31.03.2032	21.03-10.04	20	24.07.2033	51.2	7.42	19.73
18.05.2033	02.05-21.05	12	13.03.2034	30.0	11.44	33.29
15.05.2033	30.04-20.05	14	23.04.2034	92.8	9.76	28.22
12.05.2033	02.05-21.05	16	29.05.2034	176.3	8.80	24.39
10.05.2033	30.04-20.05	18	27.06.2034	277.9	8.22	21.40
08.05.2033	30.04-19.05	20	21.07.2034	392.6	7.87	19.00
25.06.2034	14.06-02.07	14	20.04.2035	408.3	11.49	27.11
23.06.2034	14.06-02.07	16	12.05.2035	596.4	10.47	23.46
22.06.2034	14.06-02.07	18	31.05.2035	805.9	9.82	20.60
20.06.2034	14.06-02.07	20	15.06.2035	1,027.9	9.37	18.30
02.08.2035	27.07-13.08	20	25.05.2036	1,960.3	11.82	17.89
31.01.2037	21.01-10.02	20	10.12.2045	3.6	10.68	32.82
03.02.2038	22.10-07.11	20	26.12.2045	3.6	9.82	30.05
03.02.2039	25.01-12.02	18	24.11.2045	3.6	10.65	32.71
06.02.2039	28.01-17.02	20	04.01.2046	3.6	9.16	27.67
03.02.2040	24.01-12.02	16	29.12.2043	3.6	11.76	35.74
07.02.2040	28.01-19.02	18	15.02.2045	3.6	9.80	29.92
10.02.2040	27.01-19.02	20	04.07.2045	3.6	8.66	25.59
06.02.2041	27.01-15.02	16	27.09.2045	3.6	10.63	32.39
09.02.2041	30.01-18.02	18	18.11.2045	3.6	9.15	27.48
11.02.2041	01.02-23.02	20	17.12.2045	3.6	8.27	23.74

* Launch window calculated considering about $+0.25$ km/s increase in ΔV_{Σ} on the boundaries of window.

Table A.2. Catalogue of selected trajectories to Sedna by the E Δ VEJSed scheme

Optimal launch date, dd.mm.yyyy	Launch window*, dd.mm	TOF, yrs	Duration of E-E trajectory part, yrs	Jupiter flyby date, dd.mm.yyyy	Height of Jupiter flyby, 10^3 km	ΔV_{Σ} , km/s	V_f , km/s
27.02.2029	16.02-20.03	16	3	03.12.2033	3.6	10.46	33.41
26.02.2029	15.02-19.03	18	3	18.09.2033	3.6	7.68	27.93
02.03.2029	18.02-22.03	20	3	29.06.2033	3.6	6.36	23.91
11.06.2030	27.05-27.06	14	3	23.03.2034	21.8	11.58	36.50
10.06.2030	26.05-26.06	16	3	30.03.2034	57.6	9.30	30.36
20.02.2030	01.02-11.03	18	2	20.09.2033	15.1	7.23	25.94
20.02.2030	01.02-11.03	20	2	16.09.2033	69.4	6.59	19.92
22.04.2031	02.04-07.05	14	2	19.03.2034	31.3	10.84	33.56
16.04.2031	22.03-26.04	18	2	30.05.2034	90.84	7.86	24.54
05.04.2031	18.03-22.04	20	2	29.06.2034	274.1	7.17	21.53
29.05.2032	14.05-18.06	16	2	21.04.2035	404.3	10.87	27.28
25.05.2032	11.05-15.06	18	2	14.05.2035	591.8	9.75	23.59
22.05.2032	08.05-13.06	20	2	02.06.2035	801.4	9.01	20.71
09.03.2037	13.02-21.03	20	3	09.11.2045	3.6	9.28	32.35
13.03.2038	18.02-26.03	20	3	29.10.2045	3.6	8.57	29.54
11.03.2039	16.02-25.03	20	3	16.07.2045	3.6	8.15	26.89
12.03.2040	17.02-26.03	20	3	05.10.2045	3.6	7.53	25.17
11.06.2041	29.05-24.06	16	3	26.04.2046	39.9	9.72	32.44
11.06.2041	29.05-24.06	18	3	29.04.2046	77.3	7.95	27.31

05.03.2041	25.02-21.03	20	3	19.08.2045	3.6	6.52	23.36
14.06.2042	26.05-22.06	14	3	14.04.2046	19.4	11.14	35.65
24.02.2042	13.02-15.03	16	3	08.01.2046	3.6	8.97	29.96
13.06.2042	27.05-21.06	18	3	19.05.2046	115.2	7.59	25.34
17.04.2042	02.04-27.04	20	3	01.07.2046	203.6	6.69	22.32

* Launch window calculated considering about +0.25 km/s increase in ΔV_{Σ} on the boundaries of window.

Table A.3. Catalogue of selected trajectories to Sedna by the E Δ VEJNSed scheme

Optimal launch date, dd.mm.yyyy	Launch window*, dd.mm	TOF, yrs	Duration of E-E trajectory part, yrs	Jupiter flyby date, dd.mm.yyyy	Height of Jupiter flyby, 10 ³ km	Height of Neptune flyby, 10 ³ km	ΔV_{Σ} , km/s	V_f , km/s
06.05.2040	30.04-10.05	18	3	11.05.2045	27.9	1.2	11.42	30.18
03.05.2040	23.04-08.05	20	3	20.05.2045	63.5	1.2	6.31	25.99
09.05.2041	02.05-13.05	18	3	11.05.2045	41.8	1.2	8.99	27.90
08.03.2041	01.03-15.03	20	3	24.06.2045	100.4	4.6	6.13	24.31
30.04.2042	22.04-07.05	17	3	21.04.2046	306.6	1.2	12.01	29.08
27.04.2042	18.04-05.05	18	3	07.05.2046	307.4	1.2	9.50	26.98
20.04.2042	12.04-28.04	20	3	04.06.2046	461.9	6.7	7.43	23.52

* Launch window calculated considering about +0.25 km/s increase in ΔV_{Σ} on the boundaries of window.

Table A.4. Catalogue of selected trajectories to Sedna by the EJNSed scheme

Optimal launch date, dd.mm.yyyy	Launch window*, dd.mm	TOF, yrs	Jupiter flyby date, dd.mm.yyyy	Height of Jupiter flyby, 10 ³ km	Height of Neptune flyby, 10 ³ km	ΔV_{Σ} , km/s	V_f , km/s
24.12.2039	22.12-12.01/40	20	23.10.2044	74.5	1.2	9.84	26.12
19.12.2040	12.12-12.01/41	20	11.08.2043	3.7	1.2	8.63	23.41
17.01.2041	08.01-27.01	18	10.12.2044	3.6	1.2	10.99	28.09
19.01.2041	09.01-27.01	20	23.01.2045	3.6	4.5	7.94	24.49
24.01.2042	15.01-12.02	18	17.12.2044	3.6	1.2	11.23	26.11
24.01.2042	15.01-12.02	20	18.12.2044	3.6	9.2	10.01	22.86
28.02.2043	20.02-11.03	18	22.02.2045	3.6	4.9	8.86	24.37
27.02.2043	18.02-09.03	20	08.02.2045	3.6	14.8	7.58	21.45
11.04.2044	30.03-18.04	15	03.05.2045	38.7	1.2	10.68	28.04
09.04.2044	30.03-18.04	16	27.05.2045	67.5	1.2	8.40	26.13
06.04.2044	27.03-16.04	18	07.07.2045	140.2	9.8	7.65	22.93
04.04.2044	25.03-14.04	20	12.08.2045	232.4	20.2	7.29	20.34
20.05.2045	08.05-27.05	15	04.05.2046	311.7	2.8	10.56	26.84
16.05.2045	06.05-26.05	18	12.06.2046	556.6	11.8	8.59	21.95
15.05.2045	05.05-25.05	20	02.07.2046	739.9	22.4	8.22	19.49
30.06.2046	21.06-09.07	16	24.04.2047	1,945.6	2.3	11.56	24.09
29.06.2046	22.06-08.07	18	10.05.2047	2,839.9	10.6	10.79	21.17
28.06.2046	23.06-06.07	20	24.05.2047	3,960.8	20.4	10.25	18.82

* Launch window calculated considering about +0.25 km/s increase in ΔV_{Σ} on the boundaries of window.

Table A.5. Catalogue of selected trajectories to Sedna by the EVEEJSed and EVE Δ VEJSed

Optimal launch date, dd.mm.yyyy	Launch window*, dd.mm	TOF, yrs	Jupiter flyby date, dd.mm.yyyy	Height of Jupiter flyby, 10 ³ km	ΔV_{Σ} , km/s	V_f , km/s
EVEEJSed						
16.11.2029	30.10-25.11	14	09.04.2034	23.0	11.77	38.92
10.10.2029	15.09-18.10	17	14.04.2034	52.2	8.21	29.60
07.10.2029	15.09-18.10	18	06.05.2034	72.6	7.42	27.39
10.11.2029	18.10-23.11	19	25.05.2034	108.7	6.72	25.28
09.11.2029	19.10-23.11	20	08.06.2034	201.0	6.27	23.60

EVEΔVEJSed						
16.11.2029	30.10-25.11	14	09.04.2034	23.0	11.77	38.92
10.10.2029	15.09-18.10	17	14.04.2034	52.2	8.21	29.60
07.10.2029	15.09-18.10	18	06.05.2034	72.6	7.42	27.39
10.11.2029	18.10-23.11	19	25.05.2034	108.7	6.72	25.28
09.11.2029	19.10-23.11	20	08.06.2034	201.0	6.27	23.60

* *Launch window calculated considering about +0.25 km/s increase in ΔV_{Σ} on the boundaries of window.*

Table A.6. Catalogue of selected trajectories to Sedna by the EJ-OM-Sed scheme

Optimal launch date, dd.mm.yyyy	TOF, yrs	Jupiter flyby date, dd.mm.yyyy	Height of Jupiter flyby, 10^3 km	ΔV_{Σ} , km/s	V_f , km/s	r_{sun}^* , 10^6 km
15.05.2029	18	07.02.2037	951.1	11.24	44.83	2.3
11.05.2029	20	28.12.2036	859.2	10.32	35.75	2.4
16.05.2030	18	14.01.2037	973.7	11.00	40.04	2.3
15.05.2030	20	09.01.2037	966.5	10.49	32.64	2.6
22.05.2031	16	06.02.2037	1,220.0	12.00	45.31	2.3
18.05.2031	18	24.12.2036	1,089.3	11.10	36.12	2.5
19.05.2031	20	10.01.2037	1,109.9	10.80	30.04	3.5
24.05.2032	16	16.01.2037	1,521.7	12.15	40.52	2.3
24.05.2032	18	19.01.2037	1,480.9	11.67	33.10	3.1
26.05.2032	20	07.02.2037	1,446.2	11.37	27.97	4.7
24.07.2035	10	06.10.2036	178.4	11.95	51.35	2.3
23.07.2035	12	20.10.2036	308.8	10.53	41.21	2.3
23.07.2035	14	30.10.2036	437.9	9.83	34.22	2.3
22.07.2035	16	11.11.2036	390.0	9.77	29.53	2.4
22.07.2035	17	30.11.2036	404.4	9.84	25.23	3.1
21.07.2035	19	14.12.2036	423.9	9.90	21.96	3.7
29.08.2036	14	17.10.2037	3.7	12.25	31.41	11.1
29.08.2036	16	18.10.2037	3.6	11.58	26.59	13.0
29.08.2036	18	23.10.2037	7.3	11.09	23.02	15.1
29.08.2036	20	31.10.2037	16.3	10.72	20.27	17.1
28.10.2038	20	24.11.2040	3.6	11.78	20.94	2.3
28.11.2039	20	28.01.2042	3.6	11.01	21.13	2.3
24.05.2040	18	18.04.2049	975.2	11.81	50.35	2.3
20.05.2040	20	17.03.2049	839.7	10.36	39.30	2.3

* *perihelion distance of the spacecraft*

References

- [1] S.S. Sheppard, THE COLORS OF EXTREME OUTER SOLAR SYSTEM OBJECTS, *Astron. J.* 139 (2010) 1394–1405. <https://doi.org/10.1088/0004-6256/139/4/1394>.
- [2] J.H. Oort, The structure of the cloud of comets surrounding the Solar System and a hypothesis concerning its origin, *Bull. Astron. Institutes Netherlands*. 11 (1950) 91–110. [https://www.mendeley.com/search/?page=1&query=The structure of the cloud of comets surrounding the Solar System and a hypothesis concerning its origin&sortBy=relevance](https://www.mendeley.com/search/?page=1&query=The+structure+of+the+cloud+of+comets+surrounding+the+Solar+System+and+a+hypothesis+concerning+its+origin&sortBy=relevance).
- [3] R. Brasser, M.E. Schwamb, Re-assessing the formation of the inner Oort cloud in an embedded star cluster – II. Probing the inner edge, *Mon. Not. R. Astron. Soc.* 446 (2015) 3788–3796. <https://doi.org/10.1093/mnras/stu2374>.
- [4] S.S. Sheppard, C.A. Trujillo, D.J. Tholen, N. Kaib, A New High Perihelion Trans-Plutonian Inner Oort Cloud Object: 2015 TG387, *Astron. J.* 157 (2019) 139. <https://doi.org/10.3847/1538-3881/ab0895>.
- [5] C. de la Fuente Marcos, R. de la Fuente Marcos, Extreme trans-Neptunian objects and the Kozai mechanism: signalling the presence of trans-Plutonian planets, *Mon. Not. R. Astron. Soc. Lett.* 443 (2014) L59–L63. <https://doi.org/10.1093/mnrasl/slu084>.

- [6] D.C. Jewitt, J.X. Luu, The solar system beyond Neptune, *Astron. J.* 109 (1995) 1867. <https://doi.org/10.1086/117413>.
- [7] M.E. Brown, D.L. Rabinowitz, C.A. Trujillo, R. Matson, M. Meyer, R. Stoss, 2004 DW, *Int. Astron. Union Circ.* 8291 (2004) 1.
- [8] M.E. Brown, C. Trujillo, D. Rabinowitz, Discovery of a Candidate Inner Oort Cloud Planetoid, *Astrophys. J.* 617 (2004) 645–649. <https://doi.org/10.1086/422095>.
- [9] J.P. Emery, C.M. Dalle Ore, D.P. Cruikshank, Y.R. Fernández, D.E. Trilling, J.A. Stansberry, Ices on (90377) Sedna: confirmation and compositional constraints, *Astron. Astrophys.* 466 (2007) 395–398. <https://doi.org/10.1051/0004-6361:20067021>.
- [10] M.A. Barucci, D.P. Cruikshank, E. Dotto, F. Merlin, F. Poulet, C. Dalle Ore, S. Fornasier, C. de Bergh, Is Sedna another Triton?, *Astron. Astrophys.* 439 (2005) L1–L4. <https://doi.org/10.1051/0004-6361:200500144>.
- [11] C.A. Trujillo, M.E. Brown, D.L. Rabinowitz, T.R. Geballe, Near-Infrared Surface Properties of the Two Intrinsically Brightest Minor Planets: (90377) Sedna and (90482) Orcus, *Astrophys. J.* 627 (2005) 1057–1065. <https://doi.org/10.1086/430337>.
- [12] M. Cuk, Resonances near the orbit of 2003 VB₁₂ (Sedna), *Proc. Int. Astron. Union.* 2004 (2004) 341–348. <https://doi.org/10.1017/S1743921304008841>.
- [13] K. Batygin, M.E. Brown, EVIDENCE FOR A DISTANT GIANT PLANET IN THE SOLAR SYSTEM, *Astron. J.* 151 (2016) 22. <https://doi.org/10.3847/0004-6256/151/2/22>.
- [14] K. Batygin, F.C. Adams, M.E. Brown, J.C. Becker, The planet nine hypothesis, *Phys. Rep.* 805 (2019) 1–53. <https://doi.org/10.1016/j.physrep.2019.01.009>.
- [15] S.J. Kenyon, B.C. Bromley, Stellar encounters as the origin of distant Solar System objects in highly eccentric orbits, *Nature.* 432 (2004) 598–602. <https://doi.org/10.1038/nature03136>.
- [16] F.C. Adams, The Birth Environment of the Solar System, *Annu. Rev. Astron. Astrophys.* 48 (2010) 47–85. <https://doi.org/10.1146/annurev-astro-081309-130830>.
- [17] N.A. Kaib, R. Roškar, T. Quinn, Sedna and the Oort Cloud around a migrating Sun, *Icarus.* 215 (2011) 491–507. <https://doi.org/10.1016/j.icarus.2011.07.037>.
- [18] E.E. Mamajek, S.A. Barenfeld, V.D. Ivanov, A.Y. Kniazev, P. Väisänen, Y. Beletsky, H.M.J. Boffin, THE CLOSEST KNOWN FLYBY OF A STAR TO THE SOLAR SYSTEM, *Astrophys. J.* 800 (2015) L17. <https://doi.org/10.1088/2041-8205/800/1/L17>.
- [19] A. Morbidelli, H.F. Levison, Scenarios for the Origin of the Orbits of the Trans-Neptunian Objects 2000 CR 105 and 2003 VB 12 (Sedna), *Astron. J.* 128 (2004) 2564–2576. <https://doi.org/10.1086/424617>.
- [20] H. Husmann, F. Sohl, T. Spohn, Subsurface oceans and deep interiors of medium-sized outer planet satellites and large trans-neptunian objects, *Icarus.* 185 (2006) 258–273. <https://doi.org/10.1016/j.icarus.2006.06.005>.
- [21] C.A. Trujillo, S.S. Sheppard, A Sedna-like body with a perihelion of 80 astronomical units, *Nature.* 507 (2014) 471–474. <https://doi.org/10.1038/nature13156>.
- [22] R. Mcgranaghan, B. Sagan, G. Dove, A. Tullos, J.E. Lyne, J.P. Emery, A survey of mission opportunities to trans-neptunian objects, *JBIS - J. Br. Interplanet. Soc.* 64 (2011) 296–303.
- [23] A.M. Zangari, T.J. Finley, S. Alan Stern, M.B. Tapley, Return to the Kuiper Belt: launch opportunities from 2025 to 2040, *J. Spacecr. Rockets.* 56 (2019) 919–930.
- [24] J. Kreitzman, C.W. Stewart, E. Cansler, J. Brisby, M. Green, J. Lyne, Mission Opportunities to Trans-Neptunian Objects—Part III, Orbital Capture, Low-Thrust Trajectories and Vehicle Radiation Environment During Jovian Flyby, in: *Adv. Astronaut. Sci.*, 2013: pp. 1487–1506. https://www.mendeley.com/catalogue/895adf6f-016f-3897-82c6-aa6a9db0d9c0/?utm_source=desktop&utm_medium=1.19.8&utm_campaign=open_catalog&userDocumentId=%7B3fcf4422-51de-4d91-9296-5fe45f1345d4%7D.
- [25] Y. Guo, R.W. Farquhar, New horizons mission design, *Space Sci. Rev.* 140 (2008) 49–74. <https://doi.org/10.1007/s11214-007-9242-y>.

- [26] C.B. Olkin, D. Reuter, A. Lunsford, R.P. Binzel, S.A. Stern, The New Horizons distant flyby of asteroid 2002 JF56, in: AAS/Division Planet. Sci. Meet. Abstr. 38, 2006: pp. 22–59.
- [27] Y. Guo, R. Farquhar, New Horizons mission design for the Pluto-Kuiper Belt mission, in: AIAA/AAS Astrodyn. Spec. Conf. Exhib., 2002: p. 4722.
- [28] K. Beisser, M. Buckley, S. Arnold, Extreme exploration and outreach: Pluto and Ultima Thule, in: Proc. Int. Astronaut. Congr. IAC, 2019.
- [29] A. Perret, Mass determination of a small body in solar system by using a test-mass during a fly-by, *Acta Astronaut.* 12 (1985). [https://doi.org/10.1016/0094-5765\(85\)90006-2](https://doi.org/10.1016/0094-5765(85)90006-2).
- [30] A. Hibberd, A.M. Hein, Project Lyra: Catching 1I/‘Oumuamua—Using Nuclear Thermal Rockets, *Acta Astronaut.* 179 (2021). <https://doi.org/10.1016/j.actaastro.2020.11.038>.
- [31] A.M. Hein, N. Perakis, T.M. Eubanks, A. Hibberd, A. Crowl, K. Hayward, R.G. Kennedy, R. Osborne, Project Lyra: Sending a spacecraft to 1I/‘Oumuamua (former A/2017 U1), the interstellar asteroid, *Acta Astronaut.* 161 (2019). <https://doi.org/10.1016/j.actaastro.2018.12.042>.
- [32] A. Hibberd, A.M. Hein, T.M. Eubanks, Project Lyra: Catching 1I/‘Oumuamua – Mission opportunities after 2024, *Acta Astronaut.* 170 (2020). <https://doi.org/10.1016/j.actaastro.2020.01.018>.
- [33] D. Sanchez, A.F. Prado, A. Sukhanov, T. Yokoyama, Optimal transfer trajectories to the haumea system, in: SpaceOps 2014 Conf., 2014: p. 1639.
- [34] D.M. Sanchez, A.A. Sukhanov, A. Prado, Optimal trajectories to Kuiper Belt Objects, *Rev. Mex. Astron. y Astrofísica*. 55 (2019) 39–54.
- [35] A. Sukhanov, A.F.B. de Almeida Prado, Use of the tethered swingby maneuver to reach the Haumea dwarf planet, *Astrophys. Space Sci.* 364 (2019) 2.
- [36] Y. Fletcher, L. N. Kaspi, N. André, Ice Giant System Exploration, White Pap. ESA 2050. (2019).
- [37] L.N. Fletcher, R. Helled, E. Roussos, G. Jones, S. Charnoz, N. André, D. Andrews, M. Bannister, E. Bunce, T. Cavalié, F. Ferri, J. Fortney, D. Grassi, L. Griton, P. Hartogh, R. Hueso, Y. Kaspi, L. Lamy, A. Masters, H. Melin, J. Moses, O. Mousis, N. Nettleman, C. Plainaki, J. Schmidt, A. Simon, G. Tobie, P. Tortora, F. Tosi, D. Turrini, Ice giant system exploration within ESA’s Voyage 2050, *Exp. Astron.* (2021). <https://doi.org/10.1007/s10686-021-09759-z>.
- [38] L.N. Fletcher, A.A. Simon, M.D. Hofstadter, C.S. Arridge, I.J. Cohen, A. Masters, K. Mandt, A. Coustenis, Ice giant system exploration in the 2020s, *Philos. Trans. R. Soc. A Math. Phys. Eng. Sci.* 378 (2020). <https://doi.org/10.1098/rsta.2019.0473>.
- [39] E. Ancona, R.Y. Kezerashvili, G.L. Matloff, Exploring the Kuiper Belt with sun-diving solar sails, *Acta Astronaut.* 160 (2019). <https://doi.org/10.1016/j.actaastro.2019.02.019>.
- [40] G. Genta, R.Y. Kezerashvili, Achieving the required mobility in the solar system through direct fusion drive, *Acta Astronaut.* 173 (2020). <https://doi.org/10.1016/j.actaastro.2020.04.047>.
- [41] P. Aime, M. Gajeri, R.Y. Kezerashvili, Exploration of trans-Neptunian objects using the Direct Fusion Drive, *Acta Astronaut.* 178 (2021) 257–264.
- [42] M. Gajeri, P. Aime, R.Y. Kezerashvili, A Titan mission using the Direct Fusion Drive, *Acta Astronaut.* 180 (2021). <https://doi.org/10.1016/j.actaastro.2020.12.013>.
- [43] V.A. Zubko, A.A. Sukhanov, K.S. Fedyaev, V. V. Koryanov, A.A. Belyaev, Analysis of Mission Opportunities to Sedna in 2029–2034, *Adv. Sp. Res.* 68 (2021) 2752–2775. <https://doi.org/10.1016/j.asr.2021.05.035>.
- [44] V.A. Zubko, A.A. Sukhanov, K.S. Fedyaev, V. V. Koryanov, A.A. Belyaev, Analysis of optimal transfer trajectories to the trans-Neptunian object (90377) Sedna, *Astron. Lett.* 47 (2021) 188–195. <https://doi.org/10.1134/s1063773721030087>.
- [45] A.A. Sukhanov, Universal solution of Lambert’s problem., *Cosm. Res.* 26 (1989) 415–423.
- [46] D. Izzo, Revisiting Lambert’s problem, *Celest. Mech. Dyn. Astron.* 121 (2015) 1–15. <https://doi.org/10.1007/s10569-014-9587-y>.
- [47] J. V Breakwell, The optimization of trajectories, *J. Soc. Ind. Appl. Math.* 7 (1959) 215–247.

- [48] J. V Breakwell, L.M. Perko, Matched Asymptotic Expansions, Patched Conics, and the Computation of Interplanetary Trajectories, in: Prog. Astronaut. Rocket., Elsevier, 1966: pp. 159–182. <https://doi.org/10.1016/B978-1-4832-2729-0.50015-6>.
- [49] A. PRADO, A comparison of the “patched-conics approach” and the restricted problem for swing-bys, Adv. Sp. Res. 40 (2007) 113–117. <https://doi.org/10.1016/j.asr.2007.01.012>.
- [50] J. Li, J. Zhao, F. Li, A new method of patched-conic for interplanetary orbit, Optik (Stuttg). 156 (2018) 121–127. <https://doi.org/10.1016/j.ijleo.2017.10.153>.
- [51] R.A.N. Araujo, O.C. Winter, A.F.B.A. Prado, R. Vieira Martins, Sphere of influence and gravitational capture radius: a dynamical approach, Mon. Not. R. Astron. Soc. 391 (2008) 675–684. <https://doi.org/10.1111/j.1365-2966.2008.13833.x>.
- [52] R.H. Battin, An Introduction to the Mathematics and Methods of Astrodynamics, Revised Edition, American Institute of Aeronautics and Astronautics, Reston ,VA, 1999. <https://doi.org/10.2514/4.861543>.
- [53] T. Eltaeib, A. Mahmood, Differential evolution: A survey and analysis, Appl. Sci. 8 (2018). <https://doi.org/10.3390/app8101945>.
- [54] M. Mitchell, An introduction to genetic algorithms. Cambridge, MA: MIT Press, 1996.
- [55] M.A. Bhatti, Practical Optimization Methods, Springer New York, New York, NY, 2000. <https://doi.org/10.1007/978-1-4612-0501-2>.
- [56] I.D. Kovalenko, N.A. Eismont, S.S. Limaye, L. V. Zasova, D.A. Gorinov, A. V. Simonov, Micro-spacecraft in Sun-Venus Lagrange point orbit for the Venera-D mission, Adv. Sp. Res. 66 (2020). <https://doi.org/10.1016/j.asr.2019.10.027>.
- [57] D.W. Dunham, R.W. Farquhar, N. Eismont, E. Chumachenko, New Approaches for Human Deep-Space Exploration, J. Astronaut. Sci. 60 (2013). <https://doi.org/10.1007/s40295-014-0025-x>.
- [58] Y. Guo, R.W. Farquhar, Baseline design of new horizons mission to Pluto and the Kuiper belt, Acta Astronaut. 58 (2006). <https://doi.org/10.1016/j.actaastro.2006.01.012>.
- [59] A.W. Case, J.C. Kasper, M.L. Stevens, K.E. Korreck, K. Paulson, P. Daigneau, D. Caldwell, M. Freeman, T. Henry, B. Klingensmith, others, The solar probe cup on the Parker Solar Probe, Astrophys. J. Suppl. Ser. 246 (2020) 43.
- [60] N. Fox, Parker Solar Probe: A NASA Mission to Touch the Sun, in: EGU Gen. Assem. Conf. Abstr., 2018: p. 10345.
- [61] B. Holler, M.T. Bannister, K.N. Singer, S.A. Stern, S.D. Benecchi, C.M.D. Ore, L.N. Fletcher, A. Guilbert-Lepoutre, C. Kiss, P. Lacerda, K.E. Mandt, M. Marsset, A.H. Parker, N. Pinilla-Alonso, D. Ragozzine, M.B. Tapley, C.A. Trujillo, O.M. Umurhan, H. Yano, L.A. Young, Prospects for Future Exploration of the Trans-Neptunian Region, Bull. AAS. 53 (2021). <https://doi.org/10.3847/25c2cfcb.5950ca1c>.
- [62] D.A. Vallado, FUNDAMENTALS OF ASTRODYNAMICS AND APPLICATIONS, J. Chem. Inf. Model. 53 (2016).
- [63] K.M. Hughes, Gravity-assist trajectories to Venus, Mars, and the ice giants: Mission design with human and robotic applications, Purdue University, 2016.
- [64] M.V. Podzolkov, I.V. Getselev, Y.I. Gubar, I.S. Veselovsky, A.A. Sukhanov, Charged particles on the Earth–Jupiter–Europa spacecraft trajectory, Adv. Sp. Res. 48 (2011) 651–660. <https://doi.org/10.1016/j.asr.2010.11.011>.
- [65] M.H. Acuna, N.F. Ness, The main magnetic field of Jupiter, J. Geophys. Res. 81 (1976) 2917–2922. <https://doi.org/10.1029/JA081i016p02917>.
- [66] Y.F. Golubev, A. V Grushevskii, V. V Koryanov, S.M. Lavrenov, A.G. Tuchin, D.A. Tuchin, Adaptive Methods of the Flybys Constructing in the Jovian System with the Orbiter Insertion Around the Galilean Moon, Sol. Syst. Res. 54 (2020) 318–328. <https://doi.org/10.1134/S0038094620040061>.
- [67] N. Divine, H.B. Garrett, Charged particle distributions in Jupiter’s magnetosphere, J. Geophys. Res. Sp. Phys. 88 (1983) 6889–6903.
- [68] J. Veverka, P. Thomas, A. Harch, B. Clark, J.F. Bell, B. Carcich, J. Joseph, C. Chapman, W. Merline, M. Robinson, others, NEAR’s flyby of 253 Mathilde: Images of a C asteroid, Science (80-.). 278 (1997) 2109–

2114. <https://doi.org/10.1126/science.278.5346.2109>.

- [69] J. Veverka, P. Thomas, A. Harch, B. Clark, J.F. Bell III, B. Carcich, J. Joseph, S. Murchie, N. Izenberg, C. Chapman, others, NEAR encounter with asteroid 253 Mathilde: overview, *Icarus*. 140 (1999) 3–16. <https://doi.org/10.1006/icar.1999.6120>.
- [70] M.J.S. Belton, C.R. Chapman, K.P. Klaasen, A.P. Harch, P.C. Thomas, J. Veverka, A.S. McEwen, R.T. Pappalardo, Galileo's encounter with 243 Ida: An overview of the imaging experiment, *Icarus*. 120 (1996) 1–19. <https://doi.org/10.1006/icar.1996.0032>.
- [71] C.C. Porco, E. Baker, J. Barbara, K. Beurle, A. Brahic, J.A. Burns, S. Charnoz, N. Cooper, D.D. Dawson, A.D. Del Genio, others, Cassini imaging science: Initial results on Phoebe and Iapetus, *Science* (80-.). 307 (2005) 1237–1242. <https://doi.org/10.1126/science.1107981>.
- [72] S.A. Stern, H.A. Weaver, J.R. Spencer, H.A. Elliott, The New Horizons Kuiper Belt Extended Mission, *Space Sci. Rev.* 214 (2018). <https://doi.org/10.1007/s11214-018-0507-4>.
- [73] M.T. Bannister, C. Shankman, K. Volk, Y.-T. Chen, N. Kaib, B.J. Gladman, M. Jakubik, J.J. Kavelaars, W.C. Fraser, M.E. Schwamb, others, OSSOS. V. Diffusion in the orbit of a high-perihelion distant solar system object, *Astron. J.* 153 (2017) 262.
- [74] R. McMillan, Spacewatch studies of the population of Earth-approaching asteroids, in: *AIAA Sp. 2001 Conf. Expo.*, 2001: p. 4657.
- [75] R.S. McMillan, *Solar System Research with the Spacewatch 1.8-m Telescope*, (2001).